

**BNL-52651
FORMAL REPORT**

**INVESTIGATION IN HARDSURFACING A
NICKEL-COPPER ALLOY
(MONEL 400)**

by

**Carl Czajkowski and Melissa Butters
Brookhaven National Laboratory
Upton, New York 11973-5000**

December 2001

ENERGY SCIENCES AND TECHNOLOGY DEPARTMENT

**Brookhaven National Laboratory
Brookhaven Science Associates
Upton, Long Island, New York 11973-5000**

**Under Contract No. DE-AC02-98CH10886 with the
UNITED STATES DEPARTMENT OF ENERGY**

BNL-52651
FORMAL REPORT

INVESTIGATION IN HARDSURFACING A
NICKEL-COPPER ALLOY
(MONEL 400)

by

Carl Czajkowski and Melissa Butters
Brookhaven National laboratory
Upton, New York 11973-5000

December 2001

ENERGY SCIENCES AND TECHNOLOGY DEPARTMENT

Brookhaven National Laboratory
Brookhaven Science Associates
Upton, Long Island, New York 11973-5000

Under Contract No. DE-AC02-98CH10886 with the
UNITED STATES DEPARTMENT OF ENERGY

DISCLAIMER

This report was prepared as an account of work sponsored by an agency of the United States Government. Neither the United States Government nor any agency thereof, nor any of their employees, not any of their contractors, subcontractors, or their employees, makes any warranty, express or implied, or assumes any legal liability or responsibility for the accuracy, completeness, or usefulness of any information, apparatus, product, or process disclosed, or represents that its use would not infringe privately owned rights. Reference herein to any specific commercial product, process or service by trade name, trademark, manufacturer, or otherwise, does not necessarily constitute or imply its endorsement, recommendation, or favoring by the United States Government or any agency, contractor, or subcontractor thereof. The views and opinions of authors expressed herein do not necessarily state or reflect those of the United States Government or any agency, contractor or subcontractor thereof.

Printed in the United States of America
Available from
National Technical Information Service
U.S. Department of Commerce
5285 Port Royal Road
Springfield, VA 22161

ABSTRACT

Brookhaven National Laboratory (BNL) investigated the causes of weldability problems and materials failures encountered with the application of Monel (Ni-Cu) 400 as a base material and Stellite 6 (Co-Cr) as the hard-surfacing material when using the oxyacetylene welding process. This work was performed under a cooperative research and development agreement (CRADA) with the Target Rock Division of the Curtiss-Wright Flow Control Corporation.

BNL evaluated two heats of Monel 400 material. One of the heats had performed well during manufacturing, producing an acceptable number of “good” parts. The second heat had produced some good parts but also exhibited a peculiar type of hardsurfacing/base metal collapse during the welding process. A review of the chemistry on the two heats of material indicated that they both met the chemical requirements for Monel 400. During examination of the failed component, linear indications (cracks) were evident on the valve body, both on the circumferential area (top of valve body) and below the hard surfaced weld deposit. Independent measurements also indicated that the two heats met the specification requirement for the material. The heat affected zone (HAZ) also contained linear discontinuities. The valve body was welded using the oxyacetylene welding process, a qualified and skilled welder, and had been given a pre-heat of between 1400-1600°F (760-871°C), which is the Target Rock qualified procedure requirement.

Both original suppliers performed mechanical testing on their material that indicated the two heats also met the mechanical property requirements of the specification.

The BNL investigation into the cause of the differences between these heats of material utilized the following techniques:

- 1) Heat Treatment of both heats of material
- 2) Hardness testing
- 3) Optical microscopy
- 4) Scanning electron microscope (SEM)/Fractography
- 5) Energy dispersive spectroscopy (EDS)

The report concludes that the cause of the failure of the valve body during welding is not obvious, however, it does not appear to be a welding issue. The observed intergranular fractures indicate a grain boundary problem. Further research is recommended.

TABLE OF CONTENTS

	<u>Page</u>
ABSTRACT	iii
EXECUTIVE SUMMARY	v
1.0 Objective/Background	1
2.0 Technical Approach.....	1
2.1 Task 1	2
3.0 Evaluation.....	2
3.1 Heat Treatments.....	6
3.2 Hardness Testing	7
3.3 Optical Microscopy	9
3.4 Scanning Electron Microscopy/Energy Dispersive Spectroscopy	34
4.0 Discussion and Conclusions	43
5.0 Recommendations for Future Research.....	45
6.0 References.....	46

EXECUTIVE SUMMARY

The goal of this material research project was to determine specific material properties for Monel 400 (nickel-copper alloy 400) that impact the ability to successfully and consistently obtain reliable hard-surfaced weld joints. Cobalt-based hard-surfacing alloys have been used in nuclear power plant components because of their excellent wear and corrosion resistance. Current and projected applications of hard-facing materials indicate that accessibility problems in valves (geometric restrictions) may preclude the use of manual or automated gas tungsten arc welding (GTAW). This affects a number of Target Rock's small globe valves that are made of Monel 400.

These valve bodies have a hard-surfaced seat that is generally made of stellite (or colmonoy) and is welded using the oxyacetylene welding (OXY) process.

The majority of valves being welded at Target Rock, with stellite, are qualified only with the oxyacetylene process. This process is highly dependent on operator skill level, and availability of qualified welders for this process is limited, as is the ability to consistently produce high quality welds without incurring material defects. There are a number of variables that are difficult to control with the current processes. These variables include:

- Base material variation (i.e., chemistry, heat treatments, processing, etc.)
- Heat input
- Hard-surfacing material type and form
- Ability to control heat application
- Accessibility to surface and material to be welded
- Control of parts positioning and weld material application
- Operator skill

BNL investigated the causes of weldability problems and materials failures encountered with the application of Monel (Ni-Cu) 400 as a base material and Stellite 6 (Co-Cr) as the hard-surfacing material when using the oxyacetylene welding process.

In order to initiate this program, it was mutually agreed (Target Rock/BNL) that BNL would evaluate two heats of Monel 400 material. One of the heats had performed well during manufacturing, producing an acceptable number of "good" parts. The second heat had produced some good parts but also exhibited a peculiar type of hardsurfacing/base metal collapse during the welding process.

During examination of the failed component, linear indications (cracks) were evident on the valve body, both on the circumferential area (top of valve body) and below the hard surfaced weld deposit. The heat affected zone (HAZ) also contained linear discontinuities. The valve body was welded using the oxyacetylene welding process, a qualified and skilled welder, and had been given a pre-heat of between 1400-1600°F (760-871°C), which is the Target Rock qualified procedure requirement.

A review of the chemistry on the two heats of material indicated that they both met the chemical requirements for Monel 400. These requirements were:

Element (wt.%)	Typical Monel 400 (Mil-N-24106)
Carbon	0.15 max.
Manganese	1.25 max.
Iron	2.50 max.
Sulfur	0.015 max.
Silicon	0.50 max.
Copper	Remainder
Nickel	63.0-70.0
Aluminum	0.50 max.
Phosphorous	0.020 max.
Lead	0.006 max.
Tin	0.006 max.
Zinc	0.02 max.

In order to verify the originally reported manufacturers' chemical analyses, Target Rock had check analyses performed by an independent laboratory on both heats. These independent measurements also indicated that the two heats met the specification requirement for the material.

Both original suppliers performed mechanical testing on their material. The results of these measurements indicated that the two heats also met the mechanical property requirements of the specification.

The only apparent difference in the two heats of material was in the heat treatments given to each, as follows:

- 1) One Heat was heat treated to 1725°F (+/-25°F), for 1 hour, 0 minutes
- 2) The second (failed) Heat was heat treated to 1420-1430°F, for 1 hour, 2 minutes

The BNL investigation into the cause of the differences between these heats of material utilized the following techniques:

- 1) Heat treatment of both heats of material
- 2) Hardness testing
- 3) Optical microscopy
- 4) Scanning electron microscope (SEM)/fractography
- 5) Energy dispersive spectroscopy (EDS)

Since the only discernible difference between the two heats of material appeared to be their final heat treatment, a series of heat treatments was performed on each heat of material. These heat treatments were intended to re-heat the specimens from a starting temperature of 1350 °F. Each of the cut samples was held at a specified temperature, ranging from 1350°F to 1750°F (in 50°F increments), for one hour. These samples were both hardness tested and then examined in

metallurgical cross-sections, after polishing and etching. The acid etchant appeared to have more aggressively attacked (preferentially etch) the specimens from the failed heat of material. The etching did not appear to be as severe in the specimens heat treated at 1550°F, 1450°F, or 1400°F. In all cases, however, there was discernible microstructure present, in addition to evidence of inclusions on some of the specimens.

There was a structural anomaly present in some of the cross-sections examined. These took the shape of circular formations that have the look of gas bubbles stopped in the middle of forming. Some of the cross-sections depict that these bubbles formed an elongated structure similar to that of a wormhole. It is unclear how these structures were formed, however they do warrant further investigation.

Scanning electron microscopy (SEM) was used to evaluate the fracture surfaces of the cracks seen in the valve body, and to analyze the pits (using EDS) seen in the photomicrographs from the optical microscopy. The fracture surface of the crack was intergranular and had various oxides present on the fracture surface. EDS revealed that the pits were composed of combinations of magnesium, calcium, and sulfur. The presence of low melting point elements on the fracture surfaces introduces the possibility of a grain boundary embrittlement issue. The EDS scans additionally displayed that oxygen (indicating an oxide film) remained quite high in all areas of the fracture. No indications of cobalt were noted in the scans. The EDS results for the base materials were reasonably consistent with the ladle and check analyses performed, with the notable exception of chromium which was present in both scans.

There were no definitive corrosive/embrittling species noted on any of the EDS examinations.

The cause of the fracture surface oxidation is still open to interpretation.

There was a definitely aggressive etchant reaction from the 1450°F heat treatment sample, which needs to be further considered.

In conclusion, the cause of the failure of the valve body during welding is not yet obvious, however, it does not appear to be a welding issue. The intergranular fractures indicate a grain boundary problem. The lack of cobalt on the fracture face seems to absolve the stellite weld metal from any grain boundary interaction.

Further research is recommended in the following areas:

- 1) The structural anomalies observed in the heat-treated specimens need to be characterized. This characterization should take the form of microhardness testing and both scanning electron microscopy and transmission electron microscopy, coupled with energy dispersive spectroscopy. Note: part of the literature survey included two documents supplied by Target Rock personnel, which indicates the possibility of a second phase formation in the presence of phosphine (PH_3) found with acetylene gas, this anomaly could be an indicator of that second phase.
- 2) The intergranular faceting of the fracture face indicates a structural problem in the material. This also needs to be further evaluated. The possibility of a graphitization

process occurring, the potential of a second phase formation, and the constituents/contaminants that may be present in the grain boundaries of this material need to be addressed. This would entail a detailed examination of grain boundaries using the transmission electron microscope coupled with a “hot stage”. The hot stage is a TEM specimen holder capable of heating the sample in the TEM, thus allowing concurrent structural examination and heat treatment “in situ”. Part of this examination will entail the search for any phosphorous using the SEM and EDS on freshly opened fracture surfaces.

- 3) Another area in need of evaluation is to quantify the actual effects of phosphine on the second phase formation in these materials. The potential embrittling/corrosive effects and their mitigation should be investigated.
- 4) The possible critical importance of the 1450°F annealing temperature, and its potential role in phosphide (Ni or Cu) eutectic formation should also be investigated.
- 5) The use of Auger electron spectroscopy (AES) is also suggested as a tool for future studies of these materials. This is a very narrowly focused technique that might provide significant information on the state of the grain boundary (e.g. contaminants, unusual elements, etc.) in this material. This type of study was performed with good results by researchers on Alloy K-500. Alloy K-500 is prone to intergranular fracture in both fatigue tests and during hot working. Although this is a different alloy, these possibilities should also be investigated for Alloy 400.
- 6) Work has been performed on the existence of intergranular strains in alloy 400 material. This work suggesting that certain crystalline orientations will develop differing strains during loading. This may allow the “alloy tailoring” of this material, through thermo-mechanical processing techniques.
- 7) Grain size plays a role in mechanical property dependence, work hardening and strain rate effects on grain boundaries in Alloy 400. This being the case, any purchase specification for manufacture of this material should specify the smallest grain size possible to obtain the minimum mechanical and weldability properties. This is perhaps another area to be evaluated (i.e., grain size dependence versus cracking susceptibility during welding).

Immediate Recommendations:

Since the literature review indicates that there is a potential corrosive effect of phosphorous compounds on the Ni-Cu material, TRC should evaluate what sources might exist for their introduction into the welding/hard-surfacing processes. These sources should be evaluated and eliminated, if possible. This would include cutting oils, solvents, and gas mixtures.

1.0 OBJECTIVE/ BACKGROUND

The goal of the material research project was to determine specific material properties for Monel 400 (nickel-copper alloy 400) that impact the ability to successfully and consistently obtain reliable hardsurfaced weld joints. Cobalt-based hard-surfacing alloys have been used in nuclear power plant components because of their excellent wear and corrosion resistance. Current and projected applications of hard-facing materials indicate that accessibility problems in valves (geometric restrictions) may preclude the use of manual or automated GTAW. This affects small globe valves that are made of Monel 400. Each valve body has a hardsurfaced seat that is generally made of stellite (or colmonoy in some cases) and is welded using the oxyacetylene welding (OXY) process. The majority of valves being welded with stellite are qualified only with the oxyacetylene process. The oxyacetylene process is highly dependent on operator skill level, and that the availability of qualified welders for this process is very limited.

The ability to consistently produce high quality welds without incurring material defects has been difficult to achieve. There are a number of variables that are difficult to control with the current processes. Defining which variable may cause a failure is critical to the development of a successful manufacturing welding process. These variables include:

- Base material variation (i.e., chemistry, heat treatments, processing, etc.)
- Heat applied
- Hardsurfacing material type and form
- Ability to control heat application
- Accessibility to surface and material to be welded
- Control of parts positioning and weld material application
- Operator skill

2.0 TECHNICAL APPROACH

The following items need to be considered for evaluation in conjunction with the current Target Rock welding process initiative for manual globe valves:

1. Base material compatibility with these processes (i.e. SST 304, Inconel 600, Monel 400)
2. Ability to hardsurface desired materials (i.e. Stellite, Colmonoy, NoRem, other material alternatives)
3. Form of hard surfacing material (i.e. Powder, Rod, Casting, Solid Insert, etc.)
4. Parameters required for acceptable deposit (eventually must meet nuclear welding requirements)
5. Number of layers required
6. Effects of preheat

7. Failure analysis of unsuccessful welds
8. Positioning control of material to be welded (hardsurfacing material and welding process)

The initial materials research that BNL investigated focused on the causes of weldability problems and materials failures encountered with the application of Monel (CuNi) 400 as a base material and Stellite 6 (CoCr) as the hardsurfacing material when using the oxyacetylene welding process.

2.1 Task 1

Analyze the material problems encountered with Monel when using the oxyacetylene welding process. One specific problem encountered is crazing of base material in the Heat Affected Zone up to 3/4" away from deposited material. Based upon the analysis and metallurgical knowledge recommend alternatives for implementation that could provide desired results. Some suggested actions or material properties that could be affecting the results are the pre-heat temperature being used and the properties of the Monel such as chemistry and microstructure.

3.0 EVALUATION

In order to initiate this program, it was mutually agreed (Target Rock/BNL) that BNL would evaluate two heats of Monel 400 material, heats 98-0396 and 99-0950. One of the heats (Inco Alloys Intl. Heat #98-0396) had performed well during manufacturing, producing an acceptable number of "good" parts. The second heat (Allvac heat # 99-0950) from a second manufacturer, had produced some good parts but also exhibited a peculiar type of hardsurfacing/base metal collapse during the welding process. Figure 1 depicts the failure mode evident after welding.

It is clear from the photograph that the material (Monel 400) appeared to have collapsed in upon itself during welding.

There were linear indications (cracks) evident on the valve body, both on the circumferential area (top of valve body) and below the hard surfaced weld deposit. The heat affected zone (HAZ) also contained linear discontinuities. The valve body was welded using the oxyacetylene welding process, a qualified and skilled welder, and had been given a pre-heat of between 1400-1600⁰F (760-871⁰C), which is the Target Rock qualified procedure requirement.

Discussions with the welder indicated that he had observed a reddish tint (liquid-like in appearance) cover the base metal during the application of the hard surfacing material. He was not specific on gas bubble formation during this operation, which would be indicative of gas trapped in the base metal. Target Rock personnel had indicated that this heat of material had been produced from double vacuum re-melted stock, which should have de-gassed the metal sufficiently to preclude gas entrapment. Ensuing conversations with Target Rock personnel indicated that although this part had failed during hard surfacing, the heat of material (Allvac 99-0950) had produced some acceptable parts for other component configurations. Other than this

particular bonnet, BNL was informed by TRC, that there were a number of “good parts” (hardsurfaced bonnets) which had been produced from this material heat.

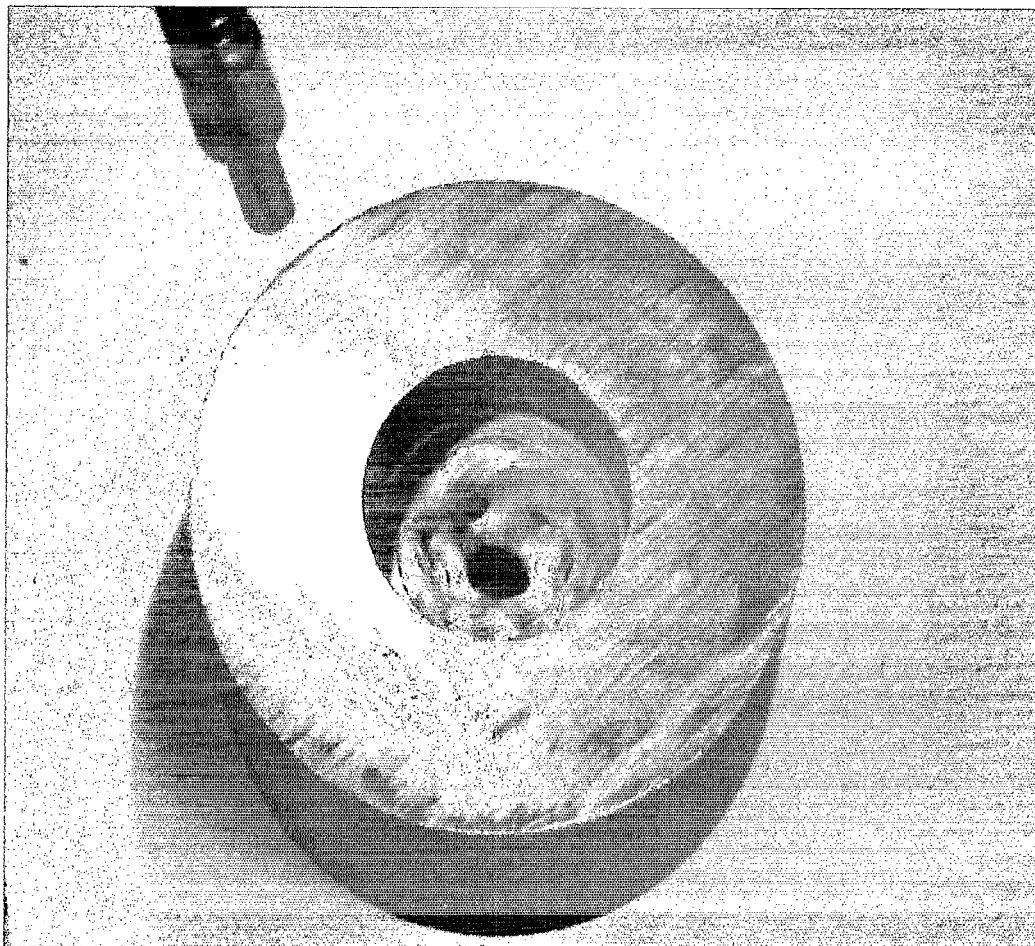


Figure 1: Digital Photograph of the Failed Valve Bonnet, After Hard-Surfacing

Table 1 is a listing of the physical properties of both cobalt and nickel alloys. It is included to demonstrate the similarities between the two alloys systems. The density, Young’s Modulus, and coefficient of thermal expansion are similar for both systems. The main differences between the two systems revolve about the crystal structure and the tensile strength (also hardness).

Table 1

	Cobalt and Cobalt Alloys (Stellites)	Nickel and Nickel alloys (Monels)
Crystal Structure	HCP below 417°C (783°F) FCC from 417°C-1493°C 783°F - 2701°F	FCC matrix with variations depending on particular grains
Density	8.8 g/cm ³	8.5 g/cm ³
Hardness	45 HRC	100 HB
Thermal Expansion Coefficient	15 μm/m·°C	13 μm/m·K
Young's Modulus	200 GPa	200 GPa
Yield Strength	550 MPa	150 MPa
Ultimate Tensile Strength	800 MPa	500 MPa

It would seem that these metals should be able to be joined together with the welding process with a minimum of difficulty. This is not necessarily the case as was shown in Figure 1.

The information provided by the certifications for each of the two heats of material evaluated for this investigation are as follows:

Table 2: Chemical Analyses (Ingot Analyses)

Element (wt.%)	Inco Heat Ingot	Allvac Heat Ingot	Typical Monel 400 Mil-N-24106
Carbon	0.14	0.12	0.15 max.
Manganese	1.02	0.87	1.25 max.
Iron	1.92	1.83	2.50 max.
Sulfur	0.001	<0.003	0.015 max.
Silicon	0.31	0.02	0.50 max.
Copper	30.89	33.21	remainder
Nickel	65.63	63.72	63.0-70.0
Aluminum	0.08	0.08	0.50 max.
Phosphorous	0.013	0.005	0.020 max.
Lead	<60 ppm	0.0003	0.006 max.
Tin	<60 ppm	0.0011	0.006 max.
Zinc	<200 ppm	0.0007	0.02 max.

It is obvious from the data presented in Table 2, that the two heats of material were of similar composition and met the specification requirements for Monel 400 (Mil-N-24106). In order to verify that the material from the two heats were in fact Monel 400, Target Rock personnel sent out samples from each heat for independent chemical analyses. Table 3 shows the result of this independent assessment:

Table 3: Chemical Analyses (Check Analyses)

Element (wt.%)	Inco Heat Check	Allvac Heat Check	Typical Monel 400 Mil-N-24106
Carbon	0.13	0.12	0.15 max.
Manganese	0.59	0.36	1.25 max.
Iron	1.82	1.64	2.50 max.
Sulfur	0.001	0.001	0.015 max.
Silicon	0.30	0.02	0.50 max.
Copper	remainder	remainder	remainder
Nickel	66.16	66.84	63.0-70.0
Aluminum	0.07	0.04	0.50 max.
Phosphorous	0.013	0.009	0.020 max.
Lead	<0.001	<0.001	0.006 max.
Tin	<0.001	<0.001	0.006 max.
Zinc	<0.01	<0.01	0.02 max.

The check analyses confirmed that both heats of material were within specification requirements and did not appear to have any marked differences between them.

Both suppliers performed mechanical testing on their material. The mechanical test data supplied follows:

Table 4: Mechanical Property Data

Property	Inco Heat	Allvac Heat
Ultimate tensile strength (psi)	83,600 (L)	82,700 (L)
	83,800 (T)	84,000 (T)
Yield strength -0.02% off. (psi)	33,700 (L)	38,100 (L)
	35,300 (T)	42,600 (T)
Elongation %	45.0 (L)	41.7 (L)
	42.7 (T)	45.5 (T)
Reduction in Area %	74.7 (L)	70.9 (L)
	67.7 (T)	72.0 (T)

Additionally, Inco reported that the room temperature Rockwell hardness for the two samples were: HRB 73 (L) and HRB 72.0 (T). Allvac did not report hardness for its material.

Both suppliers performed ultrasonic inspections of their material and found them to be acceptable.

The only apparent difference in the two heats of material was in the heat treatments given to each, as follows:

- 1) The Inco Heat was heat treated to 1725°F (+/-25°F), for 1 hour, 0 minutes
- 2) The Allvac Heat was heat treated to 1420-1430°F, for 1 hour, 2 minutes

The investigation into the cause of the differences between these heats of material utilized the following techniques:

- 1) Heat treatment of both heats of material
- 2) Hardness testing
- 3) Optical microscopy
- 4) Scanning electron microscope (SEM)/fractography
- 5) Energy dispersive spectroscopy (EDS)

The SEM is used to gather information about the surface of the samples, including the failure mode of any cracks and EDS is used to describe the composition of the sample and any inclusions found in the sample.

3.1 Heat Treatments

In order to initiate the evaluation, the valve body of the failed weld was cut in half (lengthwise), with BNL receiving $\frac{1}{2}$ of the valve body and $\frac{1}{2}$ remaining at Target Rock for archive purposes.

Two, one inch thick, four-inch diameter disks cut from bonnet material from heats Inco Alloys Intl. Heat #98-0396 and Allvac heat # 99-0950 were used for analyses during this investigation. Another sample from the Allvac heat # 99-0950 was also used for testing, however, this sample was only $\frac{1}{4}$ inch thick and had a one-inch diameter hole in the center.

The one-inch thick samples and the $\frac{1}{4}$ inch thick sample were quartered using a water-cooled, horizontal band saw. One of the quarters from a one-inch thick sample of each heat of material was cut in half again so that Inco Alloys Intl. Heat #98-0396 and Allvac heat # 99-0950 had nine individual samples prepared. The samples were labeled A through I for Inco Alloys Intl. Heat #98-0396 and 1 through 9 for Allvac heat # 99-0950. The thinner halves from heat 99-0950 were labeled H2 for heat-treated and U2 for untreated.

Since the only discernible difference between the two heats of material appeared to be their final heat treatment, it was decided (by the BNL Principal Investigator) to perform additional heat treatments on each of the newly cut specimens. These heat treatments were intended to re-heat the specimens from a starting temperature of 1350°F. Only specimen U2 was exempt from additional heat treatments. Each of the cut samples was held at a specified temperature, ranging from 1350°F to 1750°F (in 50°F increments), for one hour. Table 5 shows the heat treatment schedule and temperature attained by all samples except U2, which remained "as received".

Table 5: Heat Treatments for Monel 400

Heat (Inco)	Heat (Allvac)	Temperature (°F)
A	1 and H2	1750
B	2	1700
C	3	1650
D	4	1600
E	5	1550
F	6	1500
G	7	1450
H	8	1400
I	9	1350

3.2 Hardness Testing

Hardness testing was initiated after the completion of the heat treatments for the samples. All hardness testing was accomplished using Rockwell B methodology and using an HRB scale with a 100 kg load and a 1/16 inch ball indenter. The hardness tester was calibrated with Standard NO. 668-326, which has a hardness of HRB 72 and reported a hardness of HRB 72.5. Three hardness values were taken for each sample. Hardness testing completed all mechanical testing performed on the samples. Table 6 gives the three values obtained while testing, along with an average and standard deviation for each sample set. In general, the heat treatments affected the material in a manner consistent with accepted metallurgical tenets, i.e., samples undergoing higher heat treatments resulted in lower hardness values. Some discrepancy did arise, however, with samples A, 1, and H2, which were all heat treated to 1750°F.

These data were then plotted using a linear scale.

Figure 2 is a representation of this plot. Looking at the plot (Figure 2) is possible to see a significant dip in hardness ~11 HRB points at 1500°F, for the Allvac heat of material.

The H2 (heat treated) specimen also showed a large spread in hardness values ~21 HRB points, as did specimen A (~20 HRB points). These two specimens also had the largest deviation between datum points (Table 6). The next largest spread in data points occurred on specimen 1, which had an ~15 HRB point spread. These fairly large deviations are somewhat disturbing, since a drop in hardness is an indication of a drop in other mechanical properties (i.e. tensile strength). The copper -nickel constitutional diagram indicates that there is no eutectic or inter-metallic compound formation in this temperature region, so this “dip” in properties is still open to interpretation. Phone conversations held between BNL and Inco alloys did not shed any additional light on this apparent softening phenomenon.

Table 6: Hardness Measurements for Monel 400 After Heat Treatment

Sample	First Trial (HRB)	Second Trial (HRB)	Third Trial (HRB)	Average	Standard Deviation
A	70.0	49.2	59.2	59.4	10.4
B	66.1	67.8	63.5	65.8	2.2
C	72.0	69.0	65.5	68.8	3.2
D	69.7	73.2	70.5	71.1	1.8
E	70.5	74.9	70.0	71.8	2.7
F	69.0	72.0	74.2	71.7	2.6
G	66.5	75.4	73.0	71.6	4.6
H	67.3	73.9	75.6	72.3	4.4
I	70.1	74.5	80.0	74.9	4.9
1	35.9	51.0	47.0	44.6	7.8
2	65.0	58.0	66.5	63.2	4.5
3	68.0	60.0	62.2	63.4	4.1
4	66.9	63.8	70.0	66.9	3.1
5	57.9	60.0	64.9	60.9	3.6
6	68.6	71.9	68.5	69.7	1.9
7	74.1	69.0	69.0	70.7	2.9
8	67.0	65.9	67.5	66.8	0.8
9	80.5	72.0	69.1	73.9	5.9
H2	49.5	41.5	62.2	51.1	10.4
U2	75.3	76.0	75.0	75.4	0.5

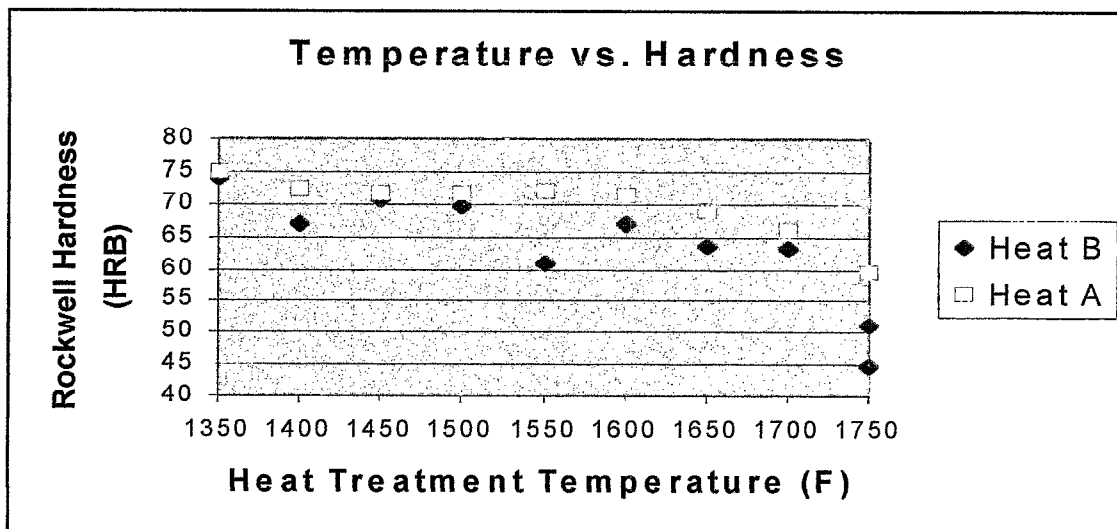


Figure 2: Relationship Between Temperature and Hardness for Heats A (Inco) and B (Allvac)

3.3 Optical Microscopy

The heat treated specimens were then cut to produce proper size samples for mounting and subsequent metallographic examination.

The same band saw used previously to quarter the samples was also used to cut the ends off of each sample so they could be taken to Curtiss Wright Flow Control-Target Rock Division in Farmingdale, New York for mounting, polishing and etching. All samples were mounted in green phenolic resin. After mounting, each sample was again labeled to maintain its unique identity.

Polishing was done using a combination of Struers RotoForce-4, RotoPol-22, Uniforce, and Multidoser. The combination of all four of these pieces of equipment was used to properly load, and polish the samples, and to evenly distribute the polishing medium. All samples were polished using the same polishing cycle, which is shown below:

1. 80 grit Struers MD Piano, with water. 90-100N force for 1.5 minutes
2. 120 grit Struers MD piano, with water. 100N force for 1.0 minutes
3. Struers MD Plan with 9 μm diamond paste. 100N force for 5.0 minutes
4. Struers MD Mol with 3 μm diamond paste. 100 N force for 4.0 minutes
5. Struers MD Nap with 1 μm diamond paste. 100N force for 1.0 minutes

Between polishing steps, the sample mount was thoroughly cleaned to remove any contaminants from the previous polishing step.

The samples were then metallurgically etched. All etching was done using a 50% -50% solution of HNO_3 (nitric acid) and H_2O (water). Each sample was held in the etchant for 20 seconds [6]. The samples were then examined using the optical microscope.

The samples prepared for microscopic examination were viewed with an optical microscope. Figures 3- 22 are the photomicrographs taken of each of the polished specimens after etching. There were a number of observations related to this part of the investigation. In general, the acid etchant appeared to more aggressively attack (preferentially etch) the specimens from the Allvac heat of material (Figures 3-11), as opposed to the etching on the Inco heat. The etching did not appear to be as severe in the specimens heat treated at 1550°F, 1450°F, or 1400°F. In all cases, however, there was a discernible microstructure present. There was also evidence of inclusions on some of the photomicrographs (Figures 4, 6, 8, 10, 11), although they were not extensive in any one specimen. Inclusions were both more prevalent and appeared to be of a larger size in the Inco heat of material (Figures 12, 13, 14, 16, 17, 18, 20, 21). The grain structure was evident in virtually all of the photomicrographs, with the exception of specimens “G”, heat treated to 1450°F, and specimen “H”, heat treated to 1400°F (Figures 18 and 19). The general attack of the specimen surface by the etchant is much more pronounced in Figure 18. A definitive grain structure re-appeared when the specimen was heat treated at 1350°F (Figure 20). Both of the “as received “ samples had a decidedly “obvious” grain structure in evidence in their photomicrographs (Figures 21 and 22). As previously stated, there are no eutectics or

intermetallic compounds found in this alloy system, so the reason for a general acid attack on the 1450°F microstructure is quite unexpected.

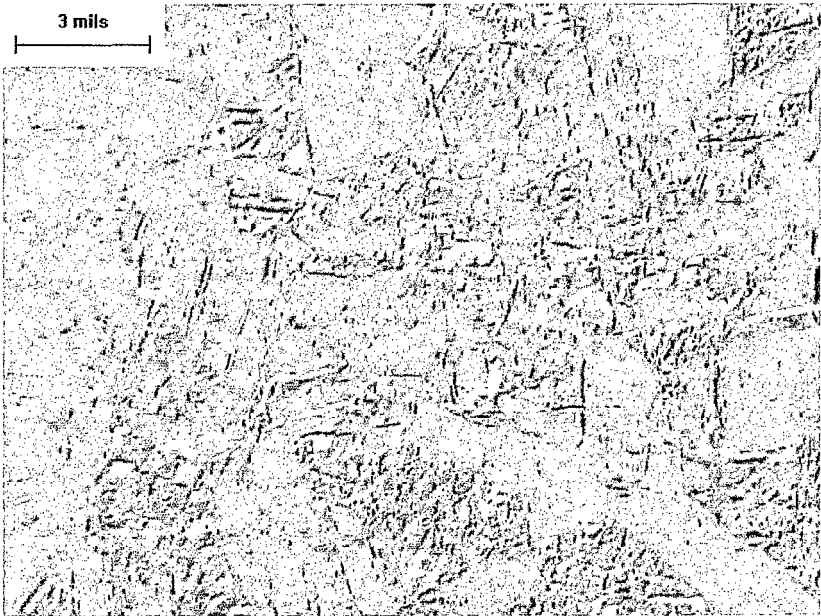


Figure 3: Optical Photomicrograph of Sample 1 (1750°F)



Figure 4: Optical Photomicrograph of Sample 2 (1700°F)

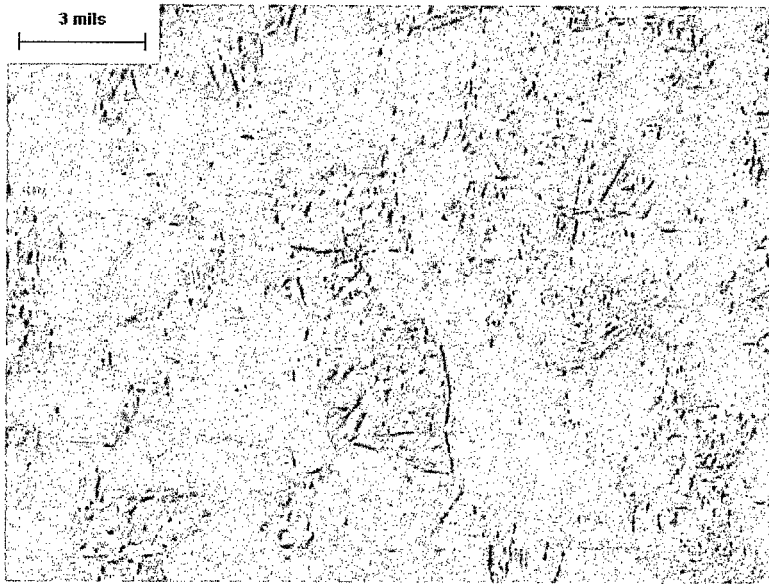


Figure 5: Optical Photomicrograph of Sample 3 (1650°F)

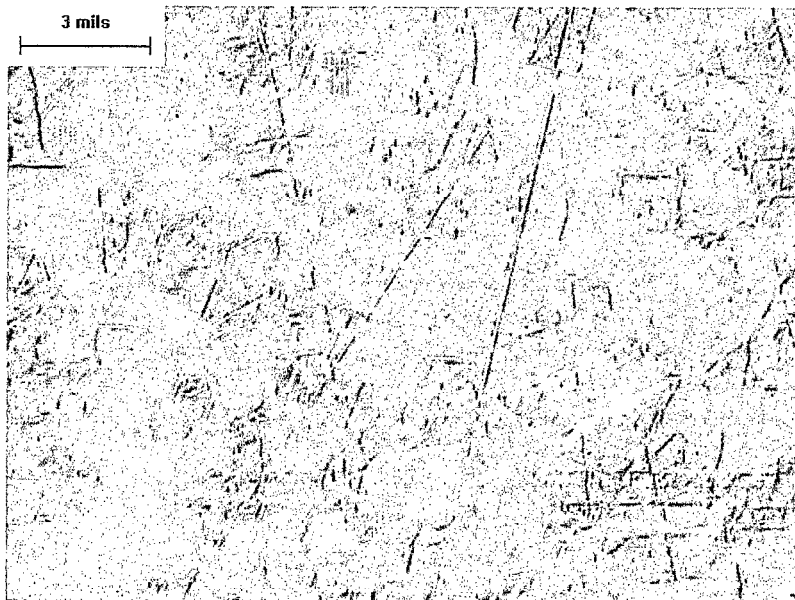


Figure 6: Optical Photomicrograph of Sample 4 (1600°F)

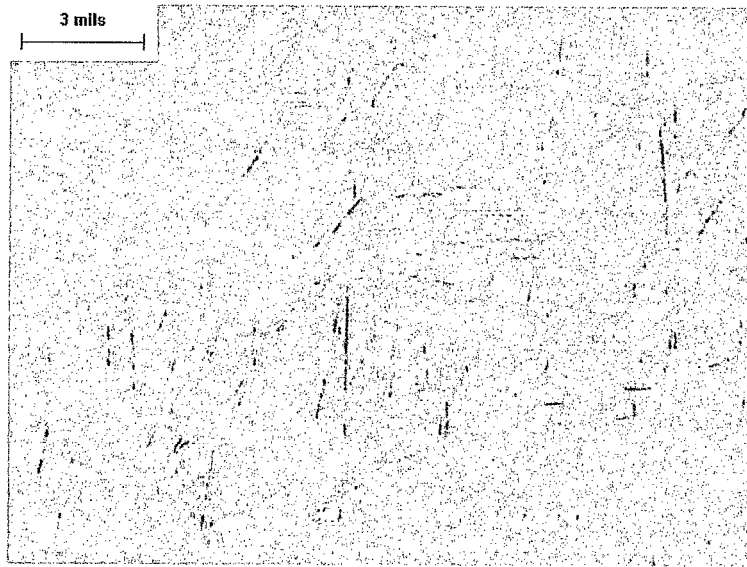


Figure 7: Optical Photomicrograph of Sample 5 (1550°F)

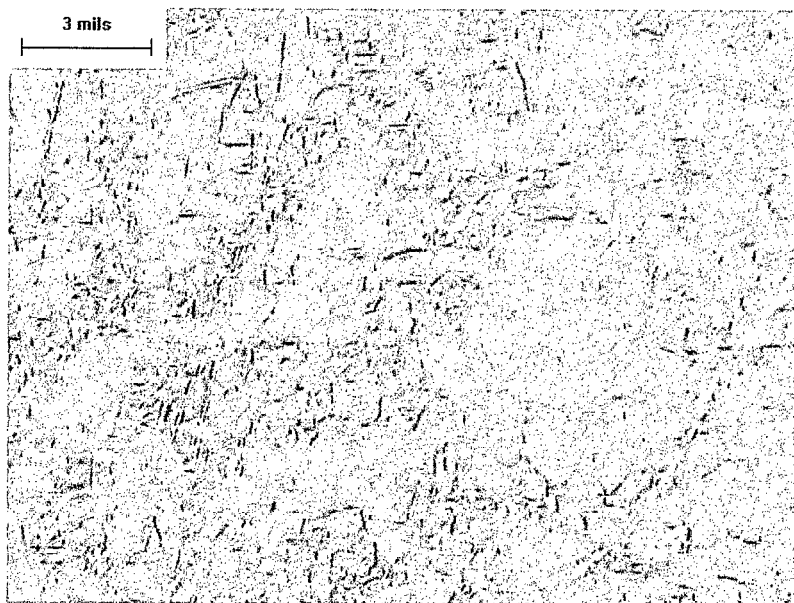


Figure 8: Optical Photomicrograph of Sample 6 (1500°F)

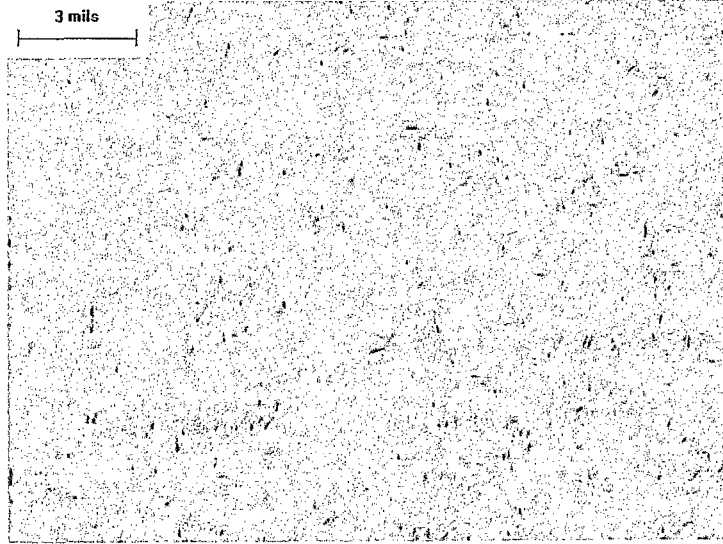


Figure 9: Optical Photomicrograph of Sample 7 (1450°F)

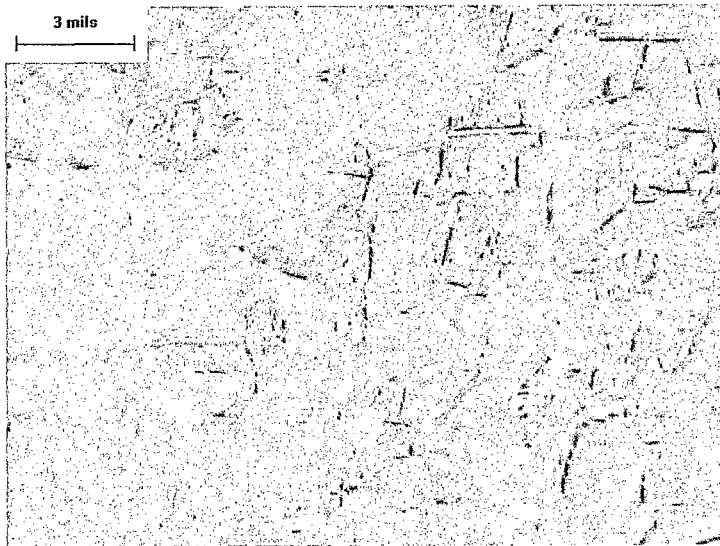


Figure 10: Optical Photomicrograph of Sample 8 (1400°F)

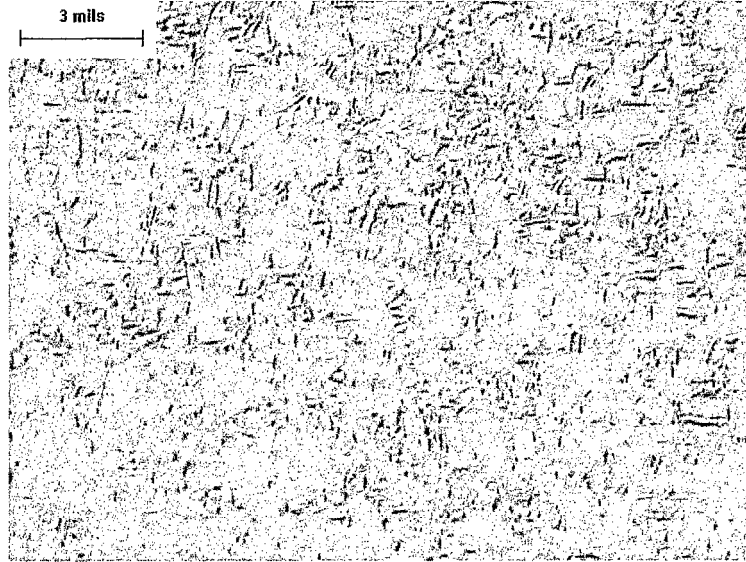


Figure 11: Optical Photomicrograph of Sample 9 (1350°F)

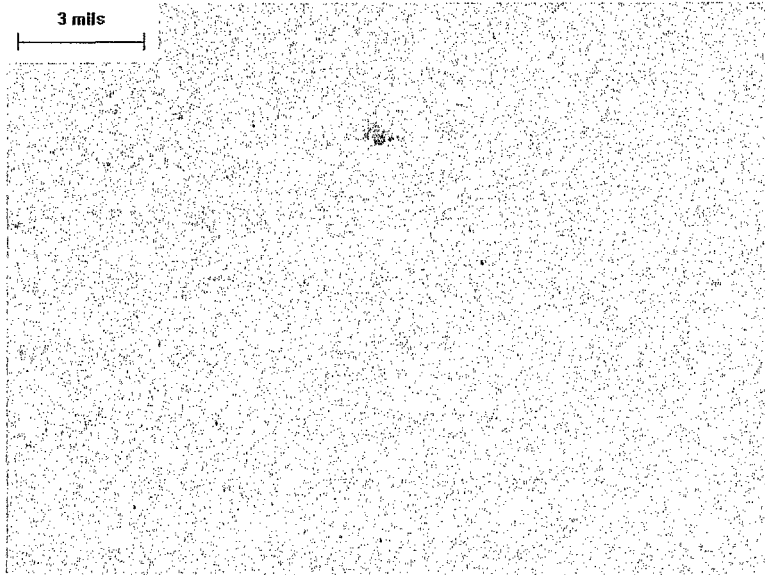


Figure 12: Optical Photomicrograph of Sample A (1750°F)

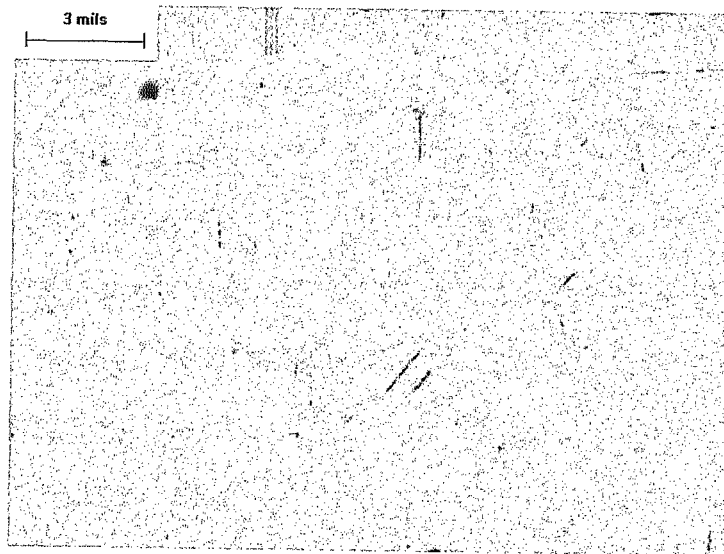


Figure 13: Optical Photomicrograph of Sample B (1700°F)

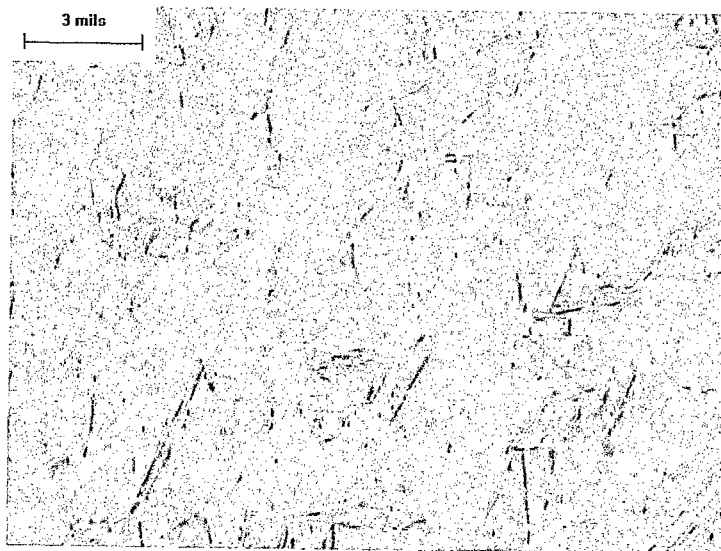


Figure 14: Optical Photomicrograph of Sample C (1650°F)

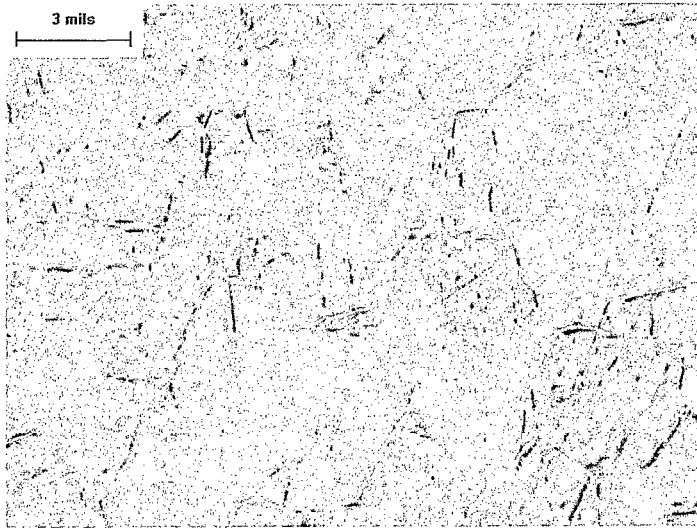


Figure 15: Optical Photomicrograph of Sample D (1600°F)

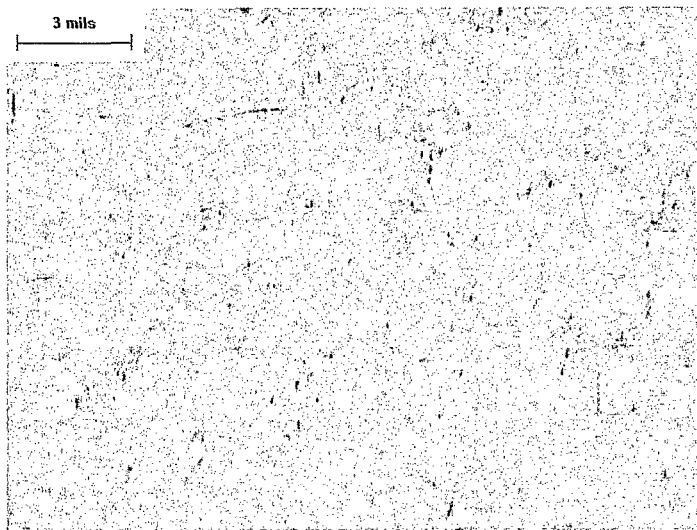


Figure 16: Optical Photomicrograph of Sample E (1550°F)

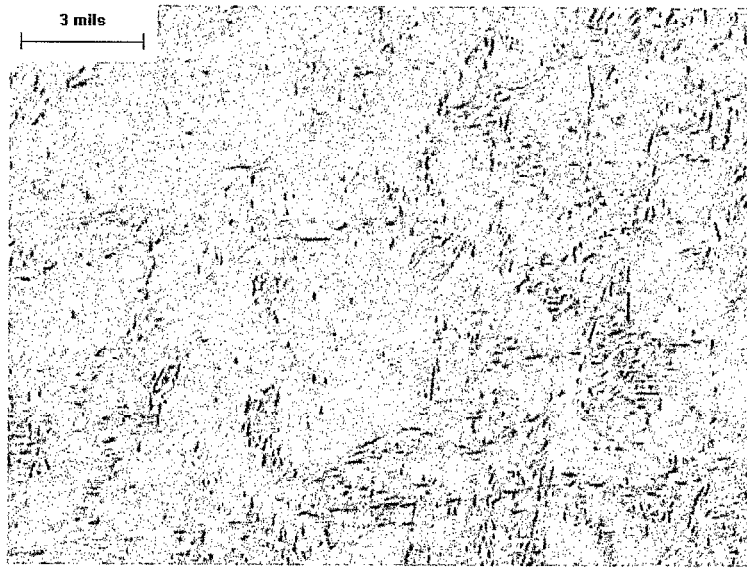


Figure 17: Optical Photomicrograph of Sample F (1500°F)

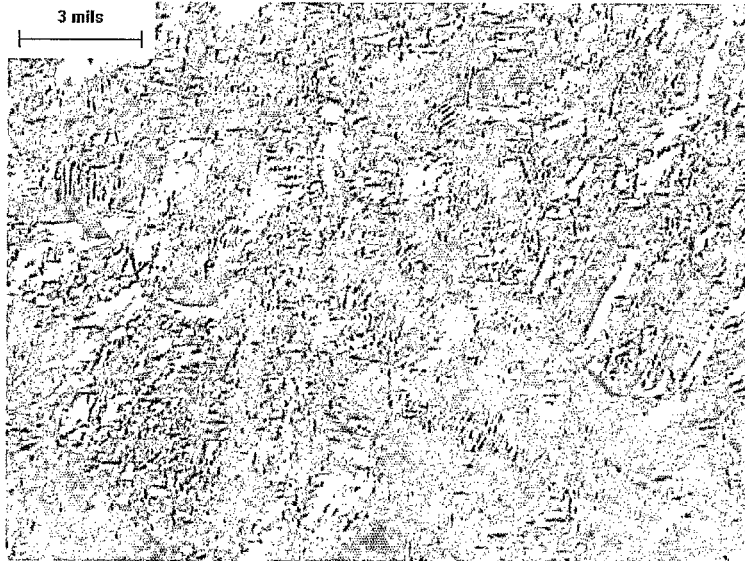


Figure 18: Optical Photomicrograph of Sample G (1450°F)

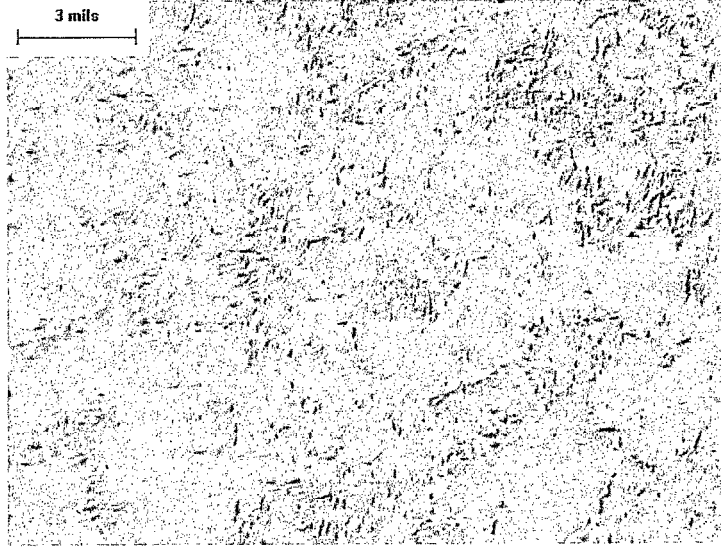


Figure 19: Optical Photomicrograph of Sample H (1400°F)

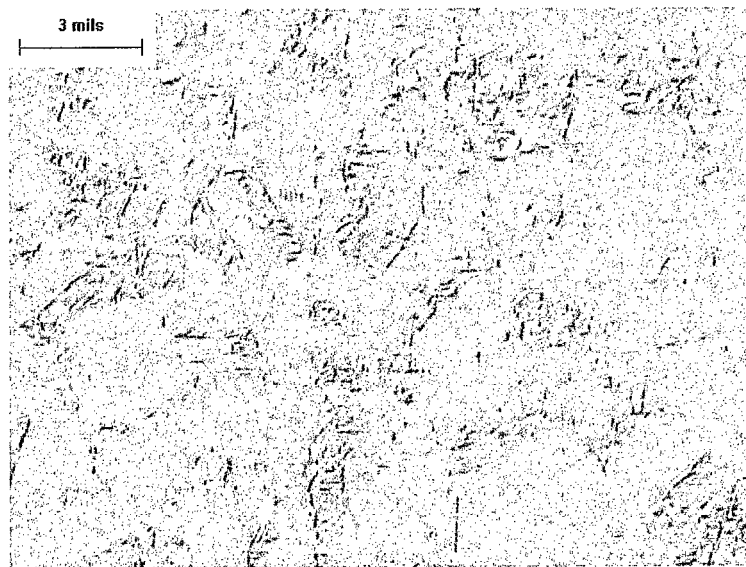


Figure 20: Optical Photomicrograph of Sample I (1350°F)

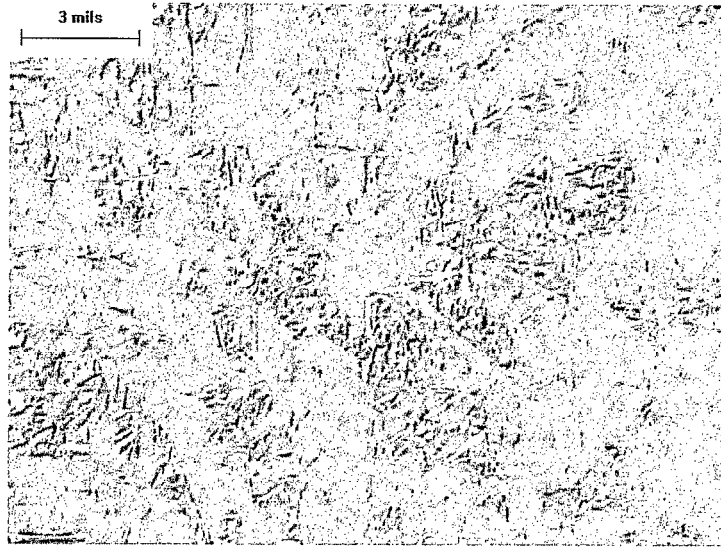


Figure 21: Optical Photomicrograph of Sample H2 (1750°F)

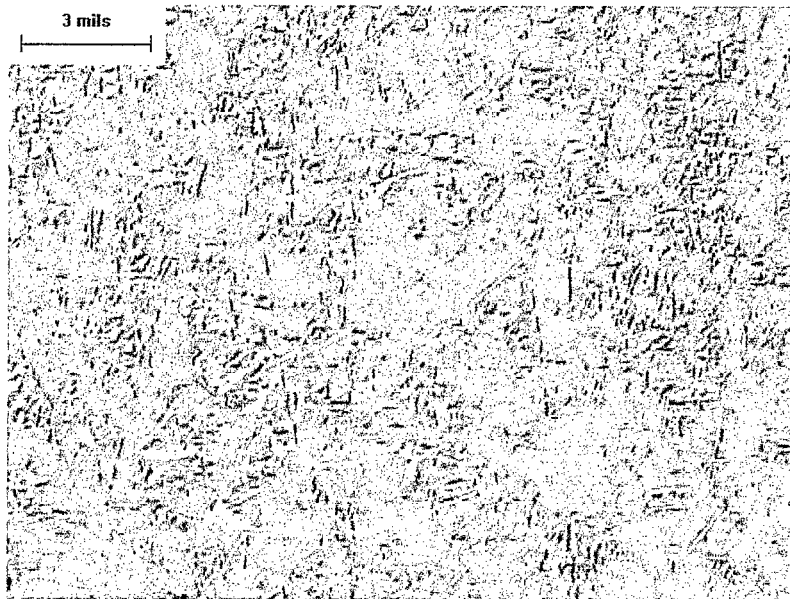


Figure 22. Optical Photomicrograph of Sample U2, “as received”, (1420 – 1430°F)

The same samples which had been previously heat treated were re-sent to Target Rock for hardsurfacing with stellite, by oxyacetylene welding. The same welder who had performed the production valve body overlay was used to do the welding. He performed the weld overlay on all of the specimens. The preheat temperatures and post weld temperatures for each of the samples are shown in Table 7.

Table 7: Pre-Heat and Post-Weld Temperature Measurements During Welding

ID	Pre-heat Temperature (°F)	Post-Weld Temperature (°F)	
		Weld	Base metal
1	1440 cooled down to 1400	1490	1432
2	1402	1459	1422
3	1531 cooled down to 1400	1630	1595
4	1400	1500	1485
5	1540 cooled down to 1400	1601	1545
6	1430	1470	1467
7	1453 cooled down to 1400	1630	1570
8	1430 cooled down to 1400	1506	1450
9	1425	1540	1506
A	1400	1545	1508
B	1450 cooled down to 1400	1452	1438
C	1422	1606	1600
D	1545 cooled down to 1400	1652	1522
E	1585 cooled down to 1400	1610	1500
F	1410	1445	1420
G	1428	1493	1480
H	1460 cooled down to 1400	1493	1422
U-small	1400-DID NOT RUN WELL (welder's comments)	1600	1545
I	1410	1450	1415

The samples were then sectioned, remounted and examined by optical microscopy. They were renamed Stellite 1, 2, 3..., and Stellite A,B,C,..., in order to maintain the same continuity of specimen identification. Figures 23-49 are the representations of the photomicrographs taken. There was no repeat of a general attack by the etchant on the surface of the specimens, however, there was a structural anomaly which appeared in a number of photomicrographs. Circular formations appear in Figures 27, 30, 45, 46, 49. They have the look of gas bubbles stopped in the middle of forming. Some of the photomicrographs depict these bubbles forming an elongated structure similar to that of a wormhole, Figures 32, 34, 43, 47, and 48. There was no attempt to analyze these structures with the SEM. This should be accomplished at a later time.

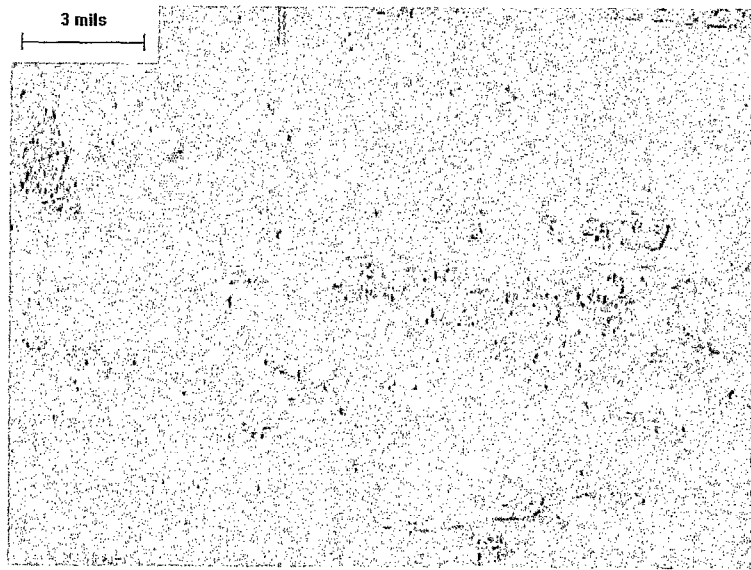


Figure 23: Optical Photomicrograph of Sample Stellite 1

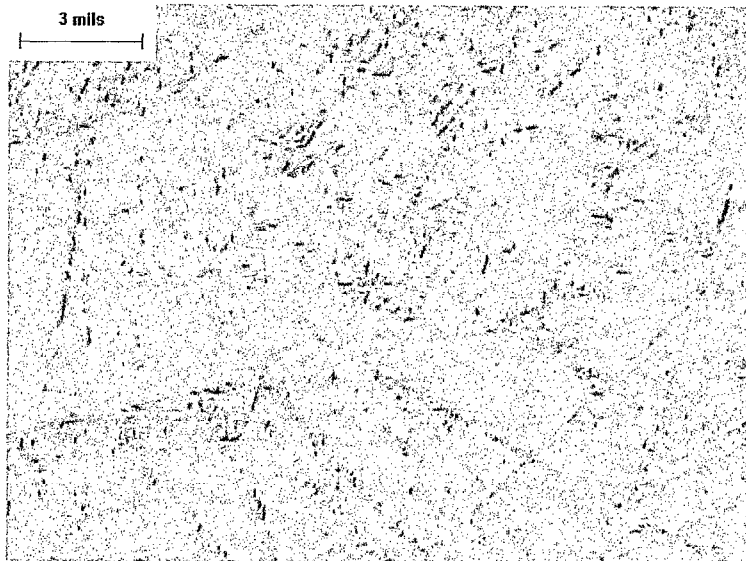


Figure 24: Optical Photomicrograph of Sample Stellite 2

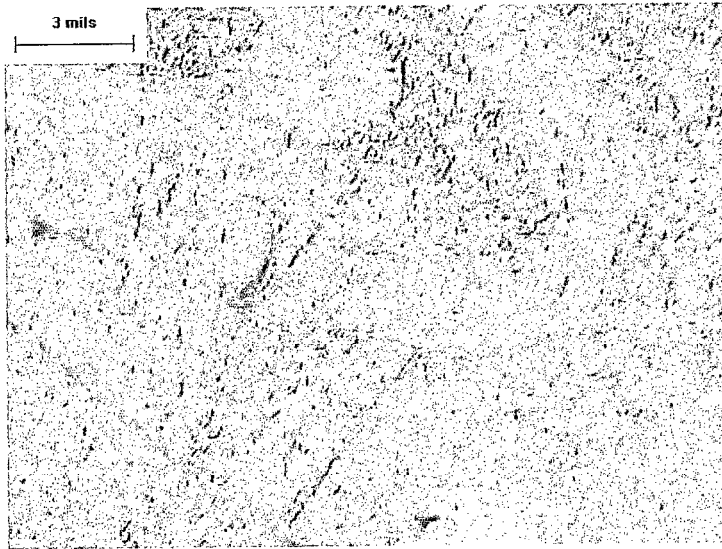


Figure 25. Optical Photomicrograph of Sample Stellite 3

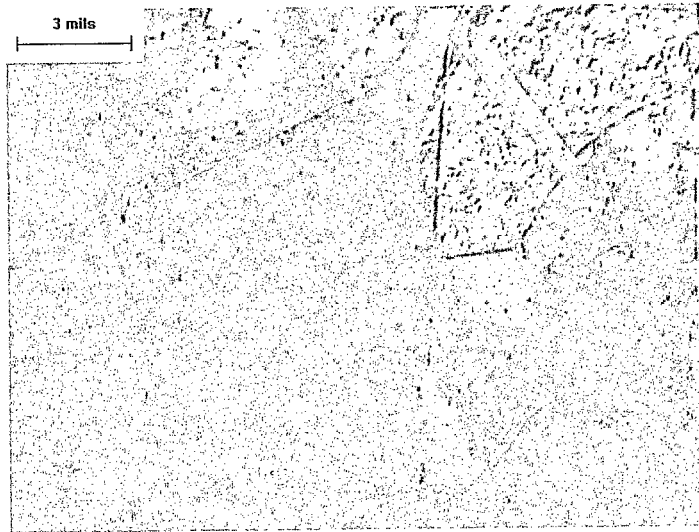


Figure 26. Optical Photomicrograph of Sample Stellite 4

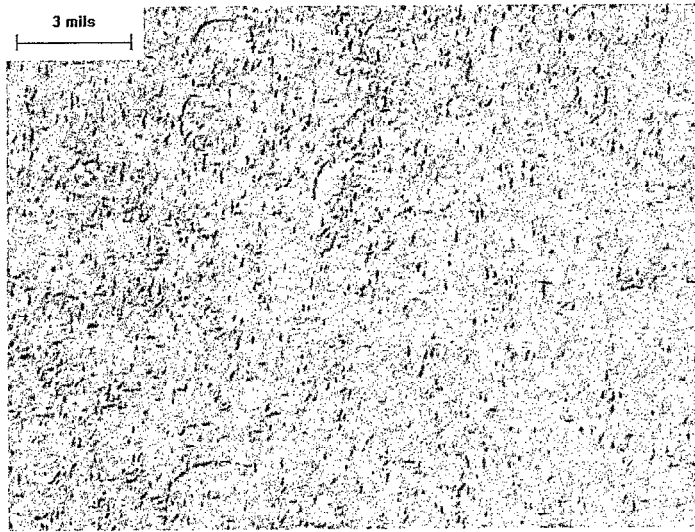


Figure 27: Optical Photomicrograph of Sample Stellite 5

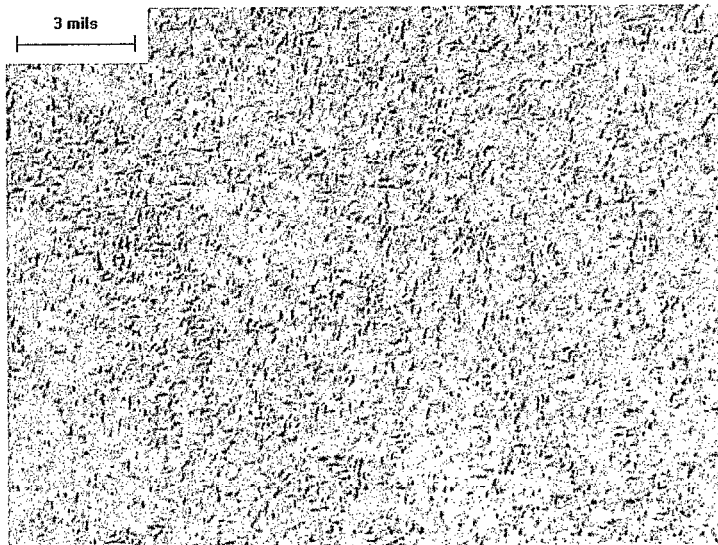


Figure 28: Optical Photomicrograph of Sample Stellite 6

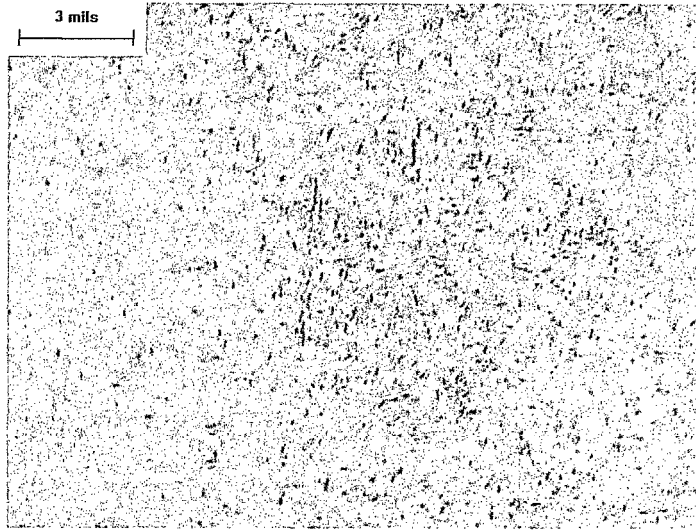


Figure 29: Optical Photomicrograph of Sample Stellite 7

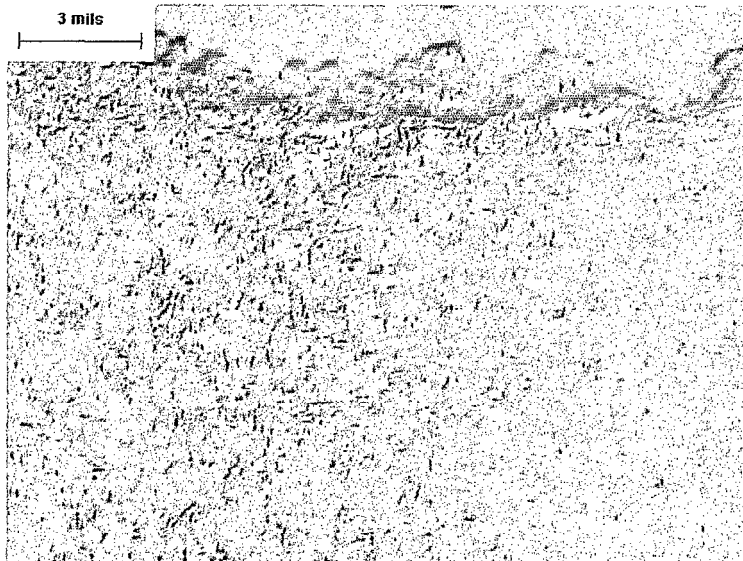


Figure 30: Second Optical Photomicrograph of Sample Stellite 7

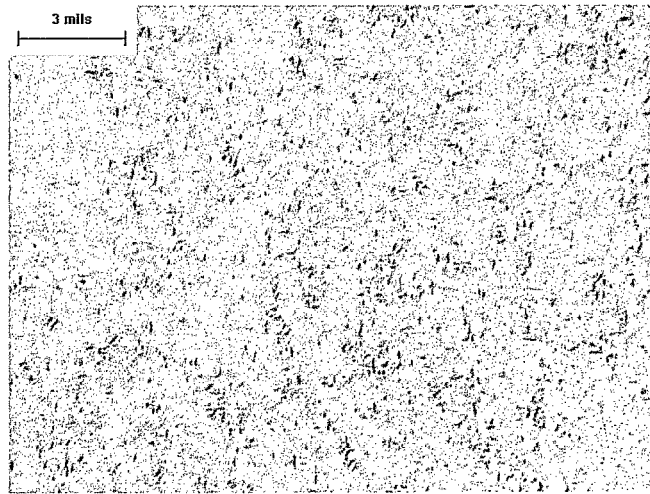


Figure 31: Optical Photomicrograph of Sample Stellite 8

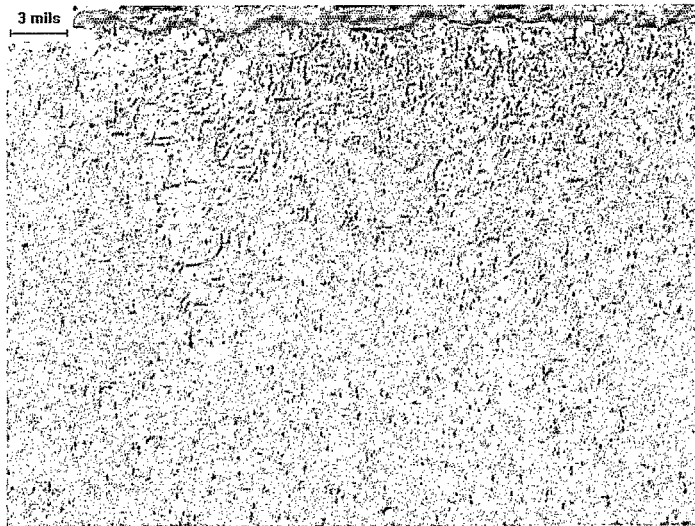


Figure 32: Second Optical Photomicrograph of Sample Stellite 8

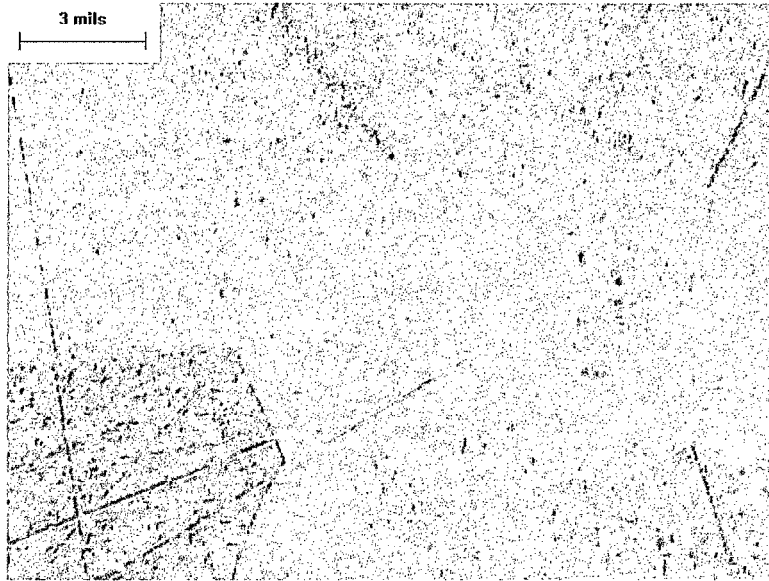


Figure 33: Optical Photomicrograph of Sample Stellite 9

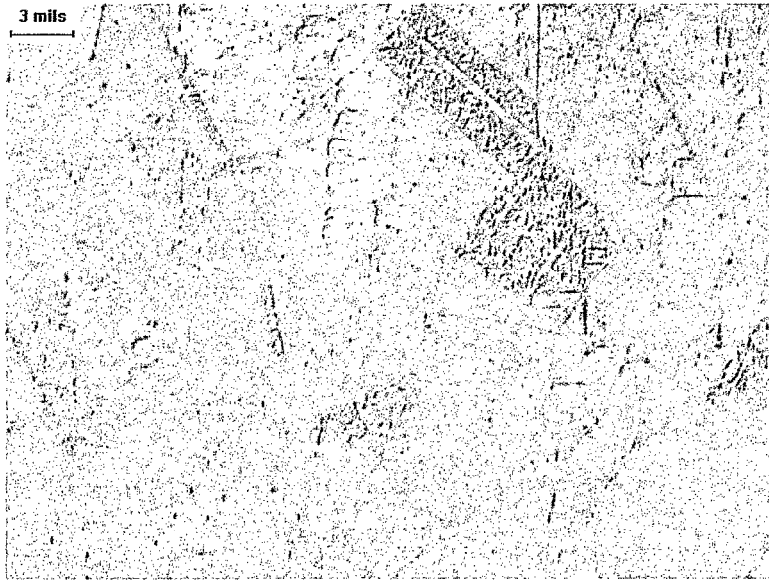


Figure 34: Second Optical Photomicrograph of Sample Stellite 9

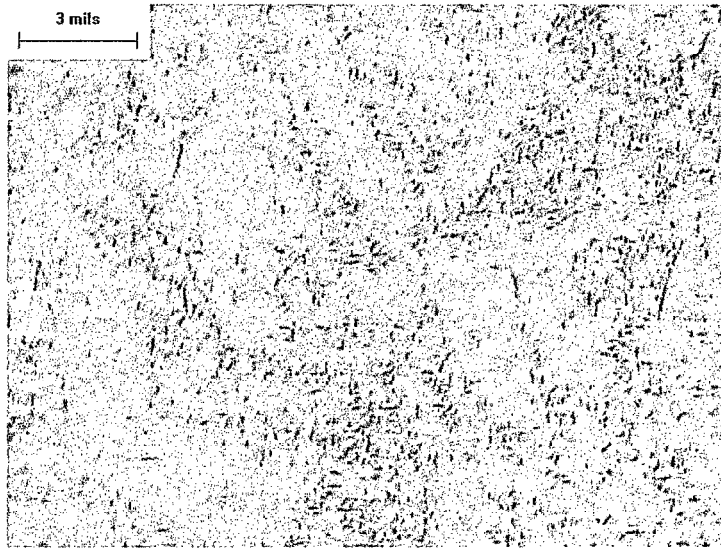


Figure 35: Optical Photomicrograph of Sample Stellite A

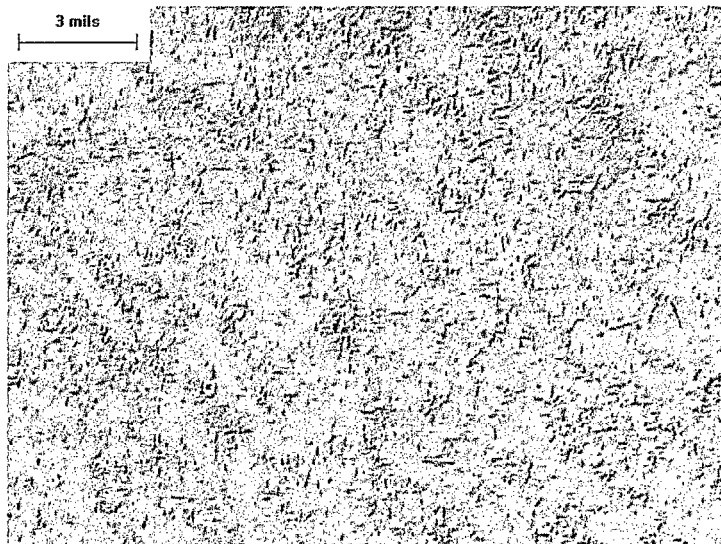


Figure 36: Optical Photomicrograph of Sample Stellite B

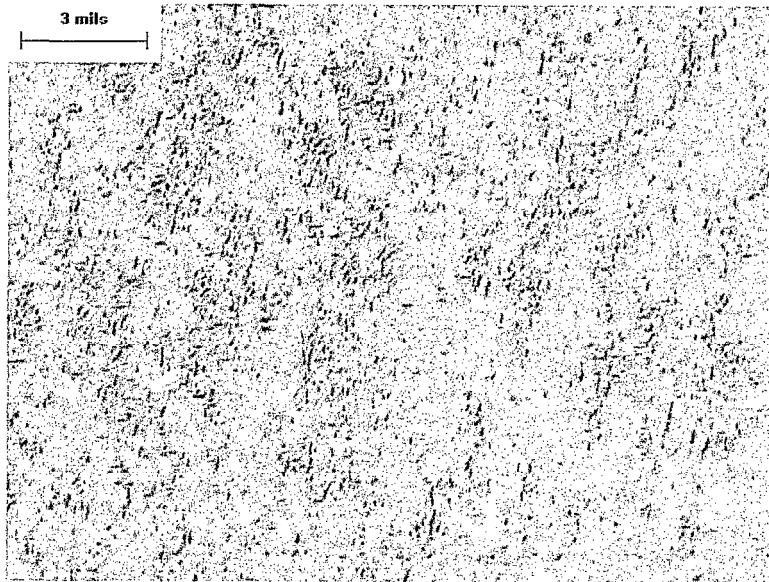


Figure 37: Optical Photomicrograph of Sample Stellite C

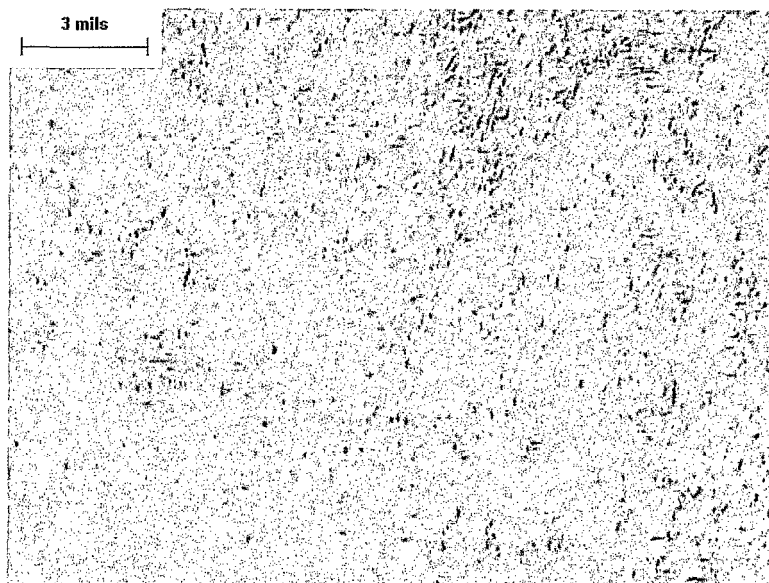


Figure 38: Optical Photomicrograph of Sample Stellite D

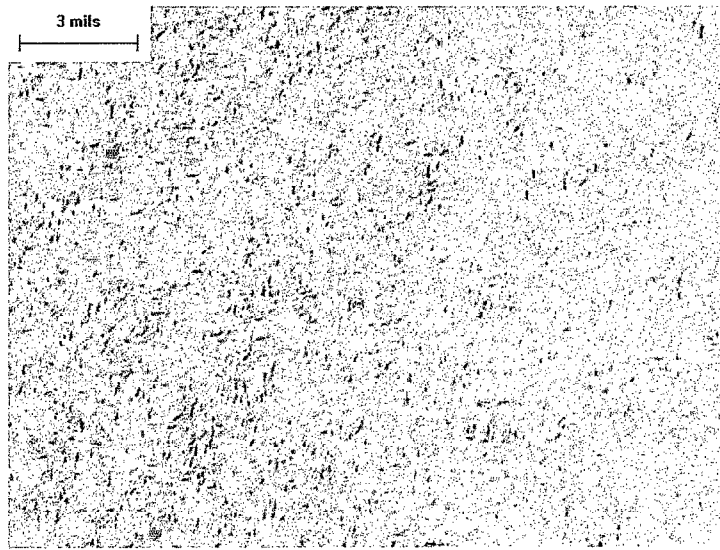


Figure 39: Optical Photomicrograph of Sample Stellite E

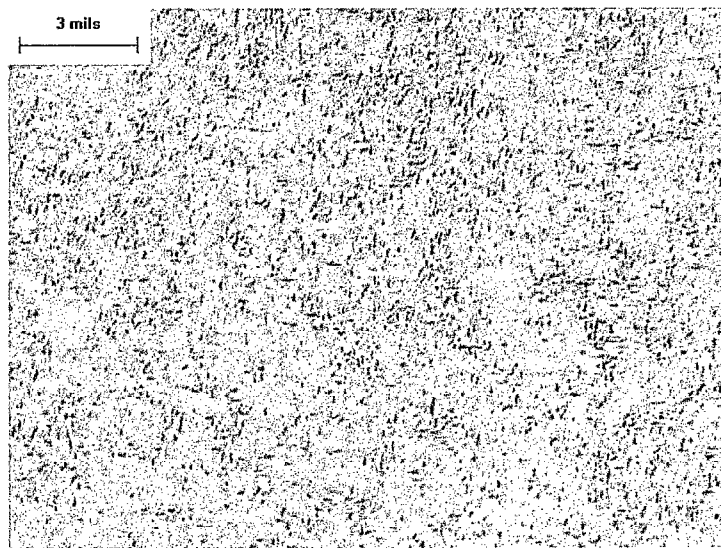


Figure 40: Optical Photomicrograph of Sample Stellite F

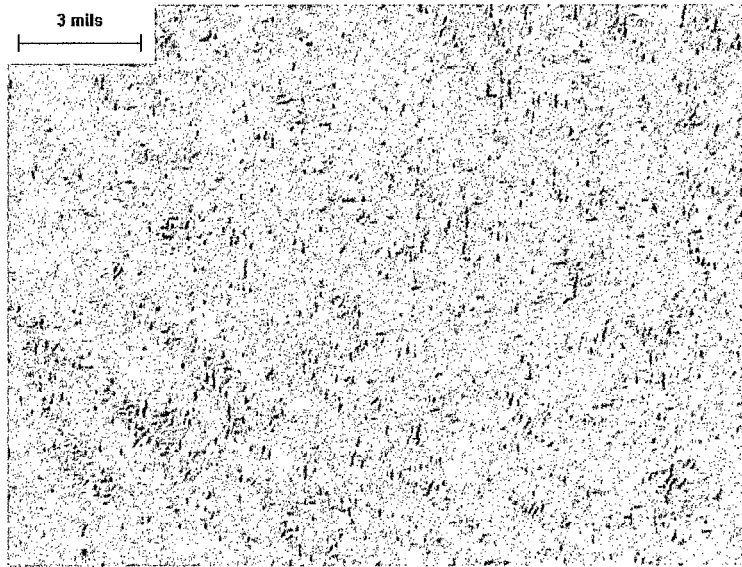


Figure 41: Optical Photomicrograph of Sample Stellite G

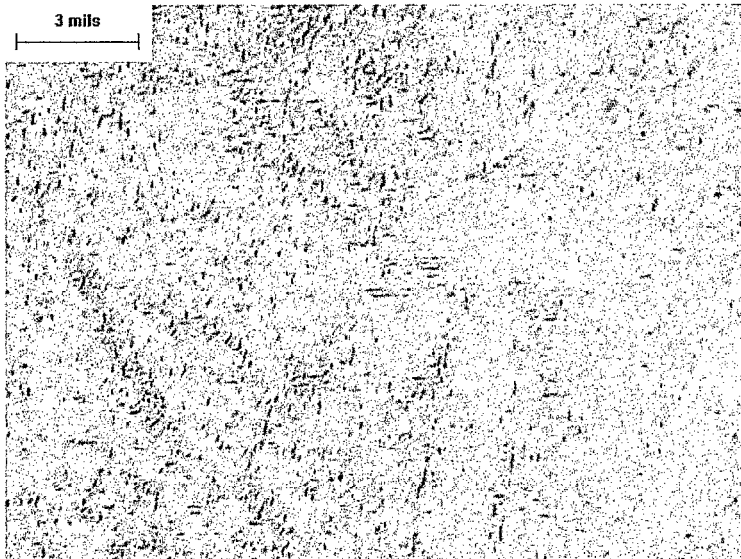


Figure 42: Optical Photomicrograph of Sample Stellite H

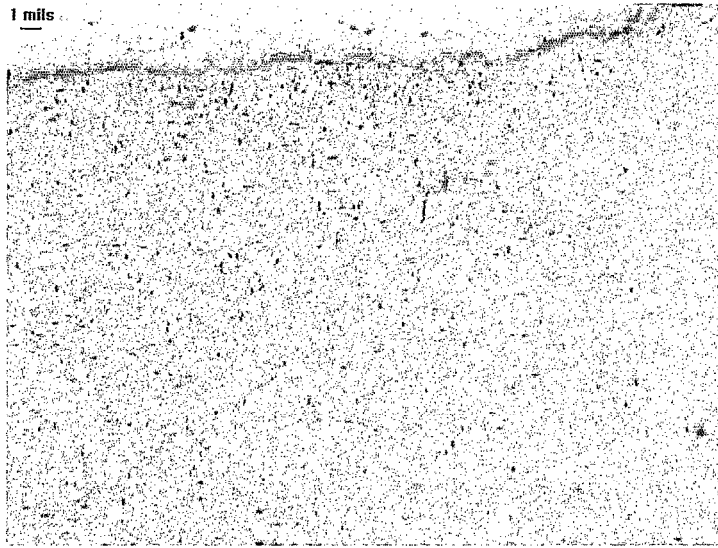


Figure 43: Second Optical Photomicrograph of Sample Stellite H

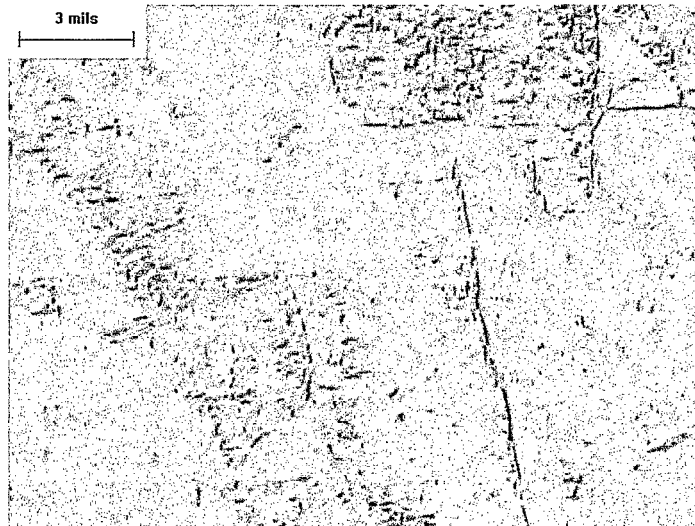


Figure 44: Optical Photomicrograph of Sample Stellite I



Figure 45: Second Optical Photomicrograph of Sample Stellite I

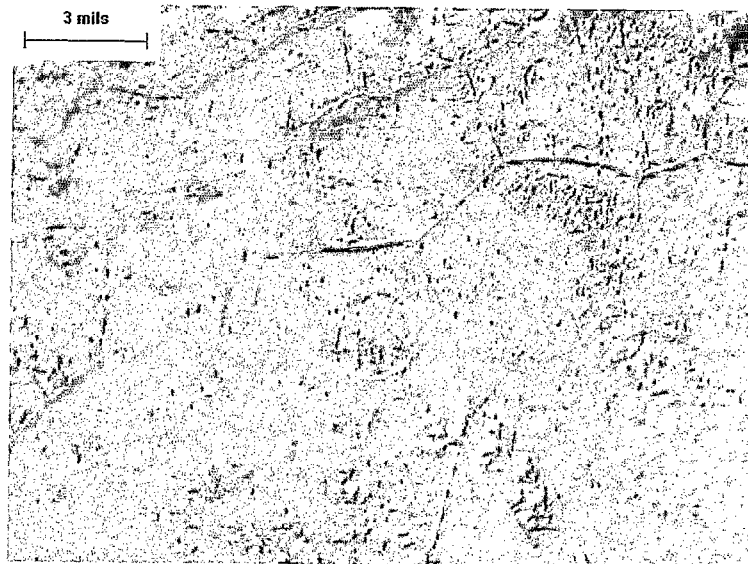


Figure 46: Third Optical Photomicrograph of Sample Stellite I

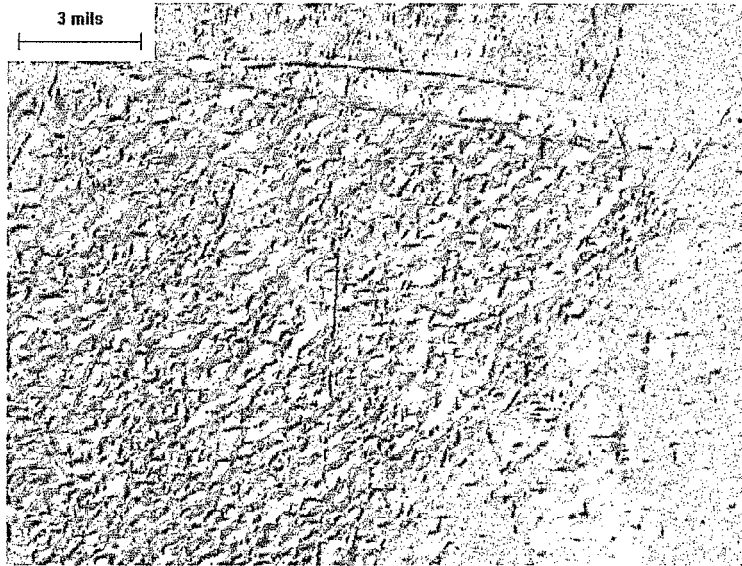


Figure 47: Optical Photomicrograph of Sample Stellite U



Figure 48: Second Optical Photomicrograph of Sample Stellite U

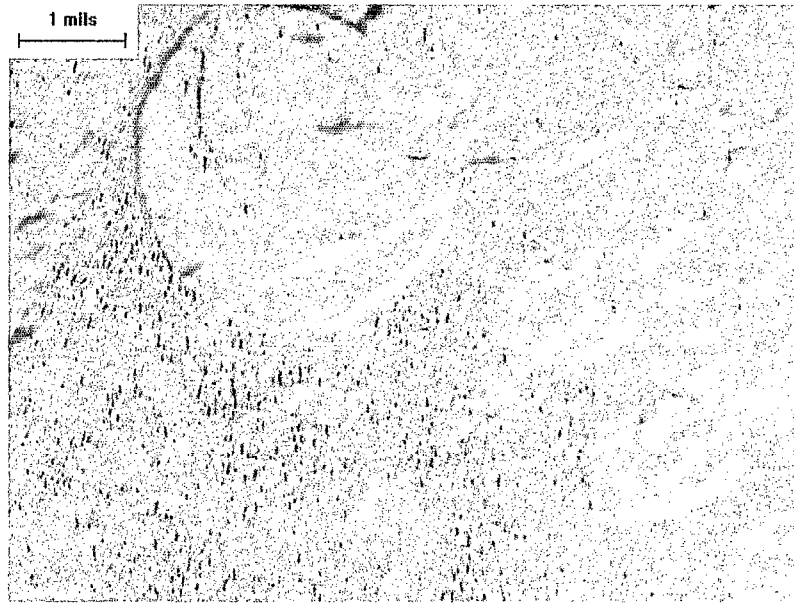


Figure 49: Optical Photomicrograph of Sample Stellite U-C

3.4 Scanning Electron Microscopy/Energy Dispersive Spectroscopy

Scanning electron microscopy (SEM) was used to evaluate the fracture surfaces of the cracks seen in the valve body from Allvac heat # 99-0950 (Figure 1) and to analyze the pits seen in the photomicrographs by optical microscopy. Chemical analyses were performed using energy dispersive spectroscopy (EDS).

EDS is an analytical technique capable of performing elemental analysis of micro-volumes typically of a few cubic microns in bulk samples and considerably less in thinner sections. Analysis of X-rays emitted from a sample is accomplished by crystal spectrometers which used energy dispersive spectrometers and permit analysis by discriminating among x-ray energies.

The feature of electron beam microanalysis that best describes this technique is its mass sensitivity. For example, it is often possible to detect less than 10^{-16} of an element present in a specific micro-volume of a sample. The minimum detectable quantity of the given element or its detectability limit varies by many factors, and in most cases is less than 10^{-16} grams/micro-volume.

EDS revealed that the pits visible were composed of combinations of magnesium, calcium, and sulfur (Figures 50, 50a, 51, and 51a). These elements were not included in the original chemical analyses for either heat of material. The fracture surfaces of the crack (Figures 52, 52a, 53, 53b, 53c, 53d, 53e) indicated the crack was intergranular (Figures 52 and 53) and had various oxides present on the fracture surface. As the EDS scan moved deeper into the crack (away from the outside free surface), the values for oxygen (indicating an oxide film) remained quite high (Figures 53a-e). There was no indication that the fracture surfaces had been affected by the weld metal being used since no indications of cobalt were noted in the scans. Figures 54 and 55 are

semi-quantitative EDS scans of the two materials to verify the chemical constituents of the two heats of material. The EDS results were reasonably consistent with the ladle and check analyses performed, with the notable exception of chromium which was present in both scans.

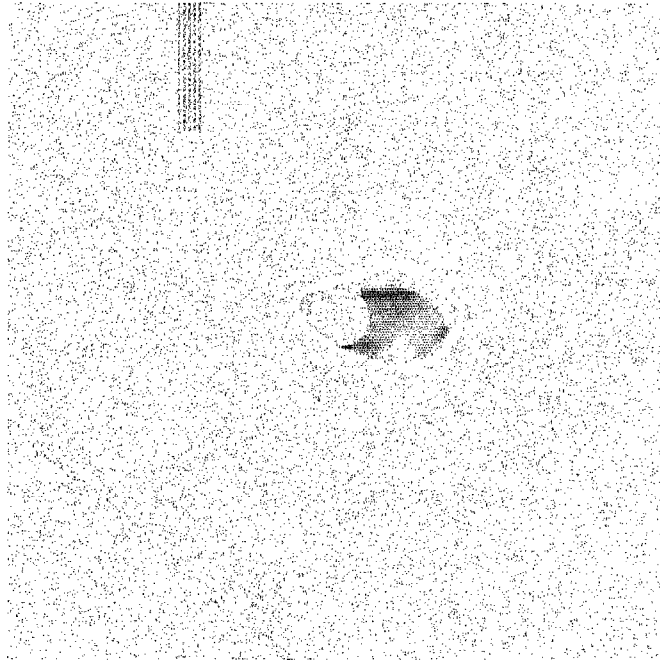


Figure 50: SEM Photomicrograph of a Pit Seen by Optical Microscopy, Revealing an Inclusion

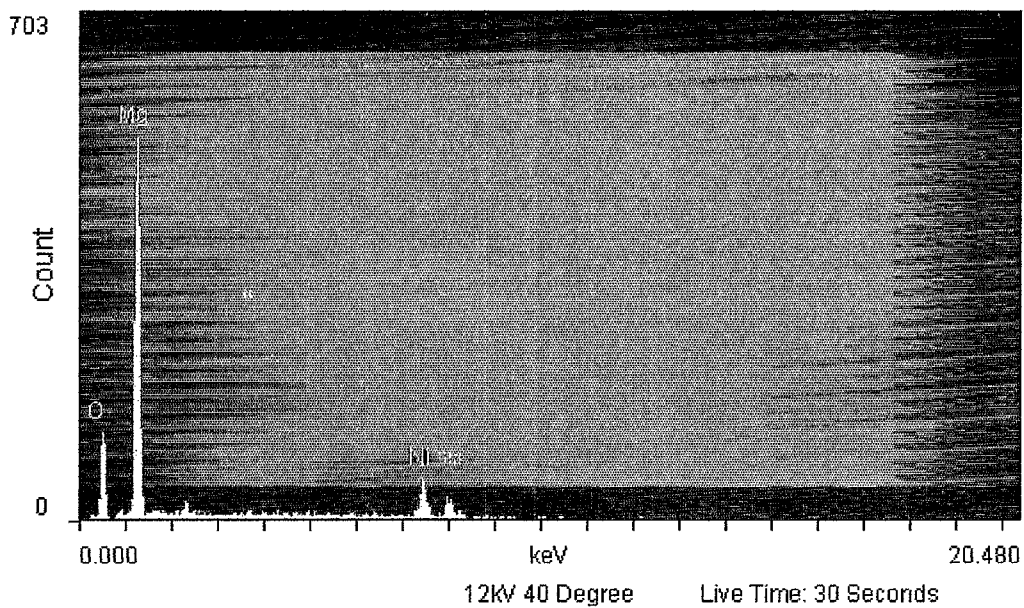


Figure 50a: EDS scan of Pit constituents

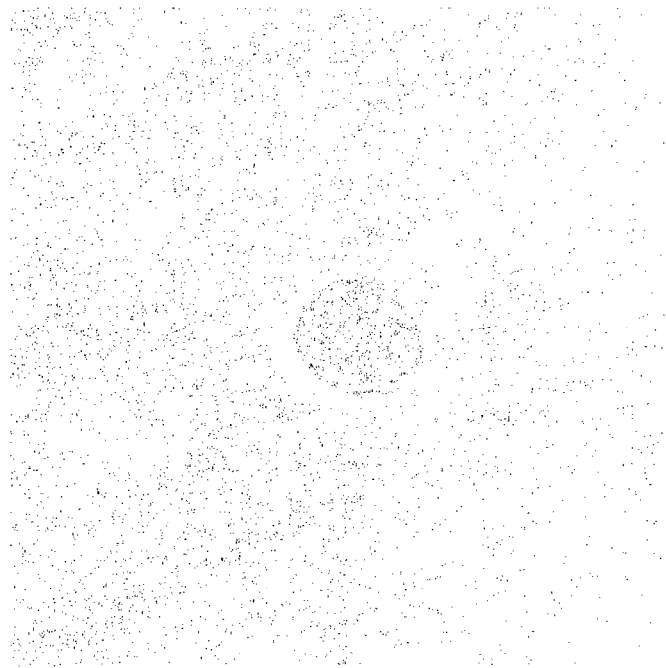


Figure 51: SEM Photomicrograph of Second Inclusion Examined

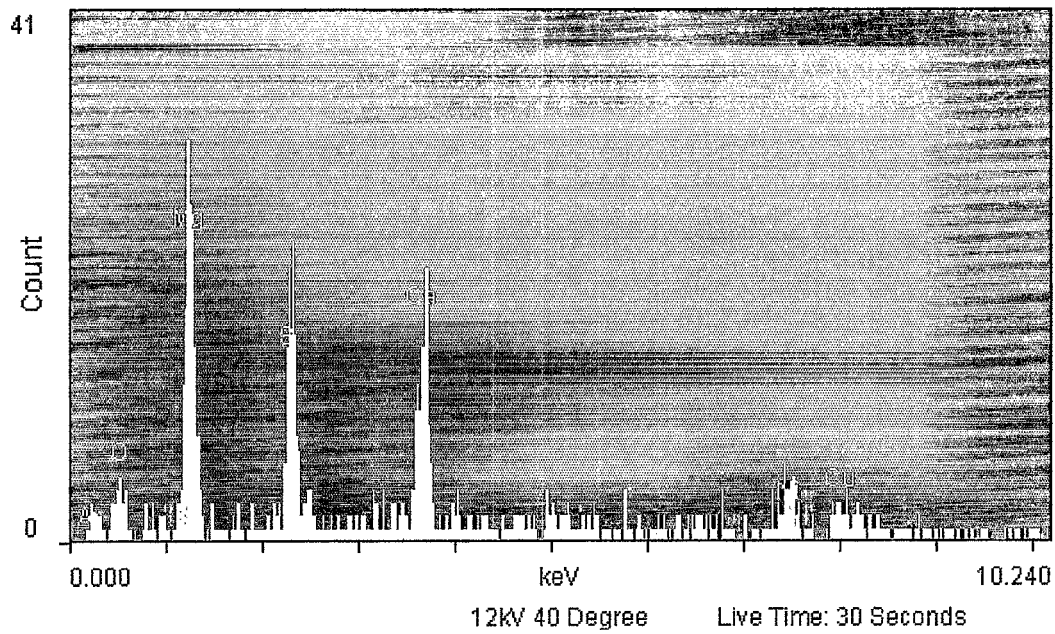


Figure 51a. EDS scan of second pit for chemical constituents

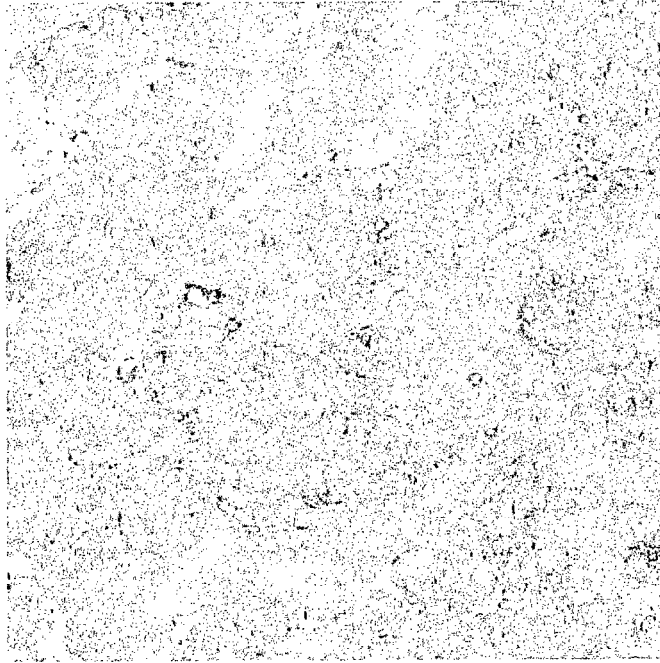


Figure 52: SEM fractograph of Surface of Crack from the Failed Valve Body Definitely Intergranular in Appearance

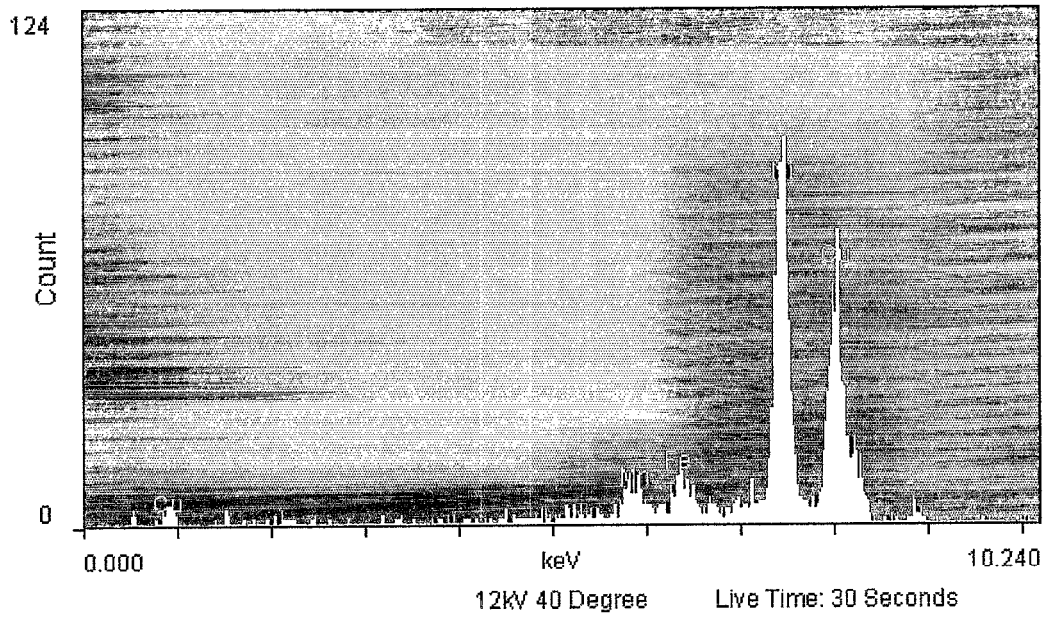


Figure 52a: EDS Scan of Fracture Face, Denoting Chemical Constituents

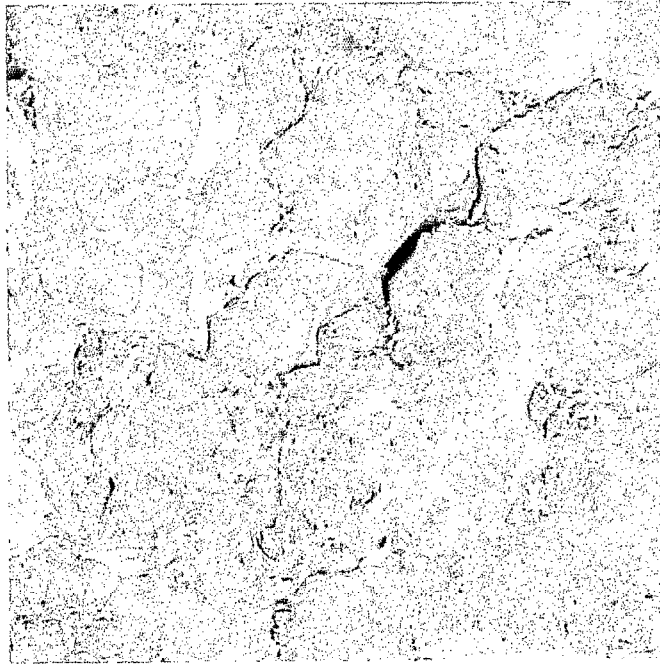


Figure 53: Intergranular Features are Very Distinct in this Fractograph of a Second Area Examined

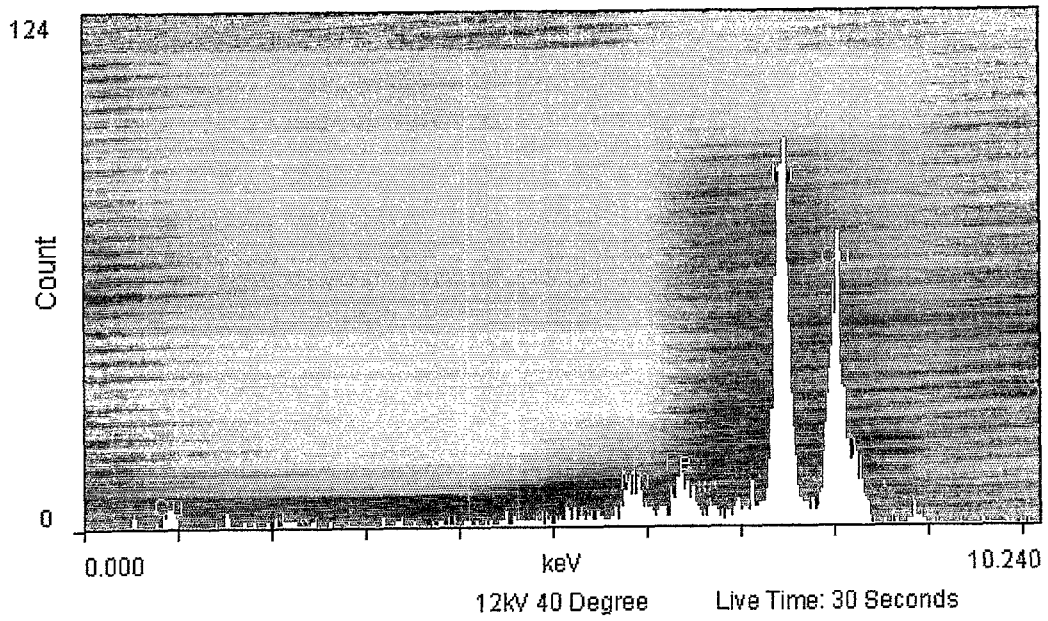


Figure 53a: EDS Scan of Second Area of Crack Examined (Figure 53)

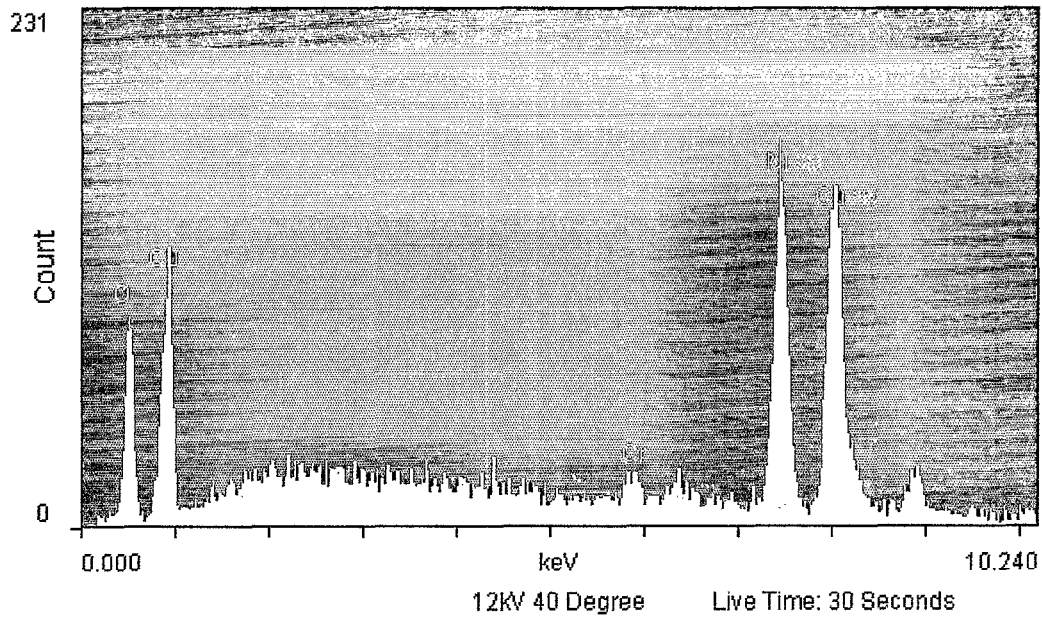


Figure 53b: Third Area of Crack Examined by EDS

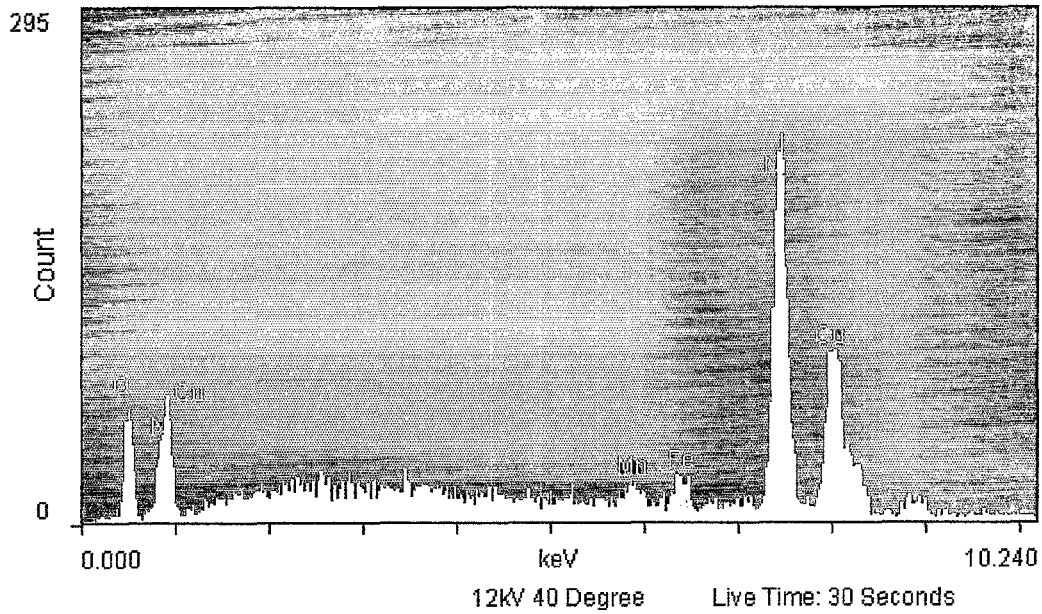


Figure 53c: Fourth Area of Crack Examined by EDS

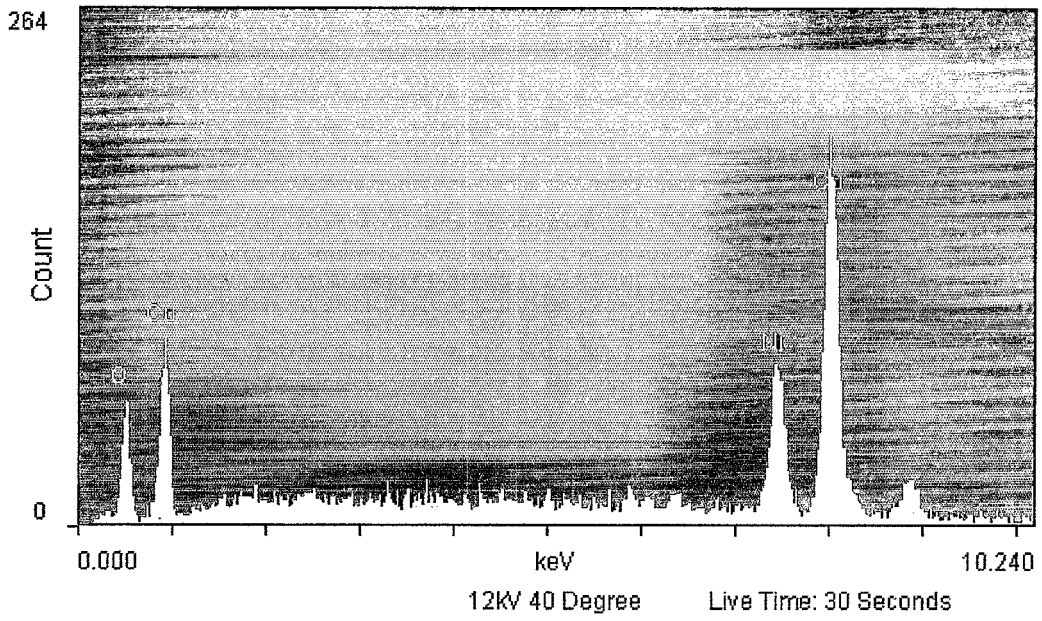


Figure 53d: EDS Spectra of Another Area of the Fracture

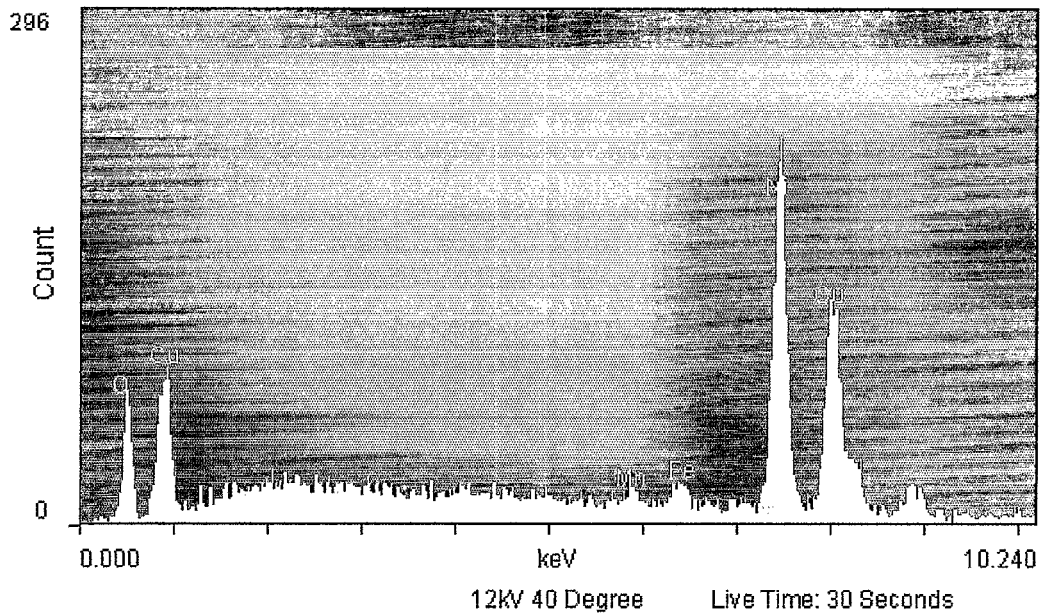
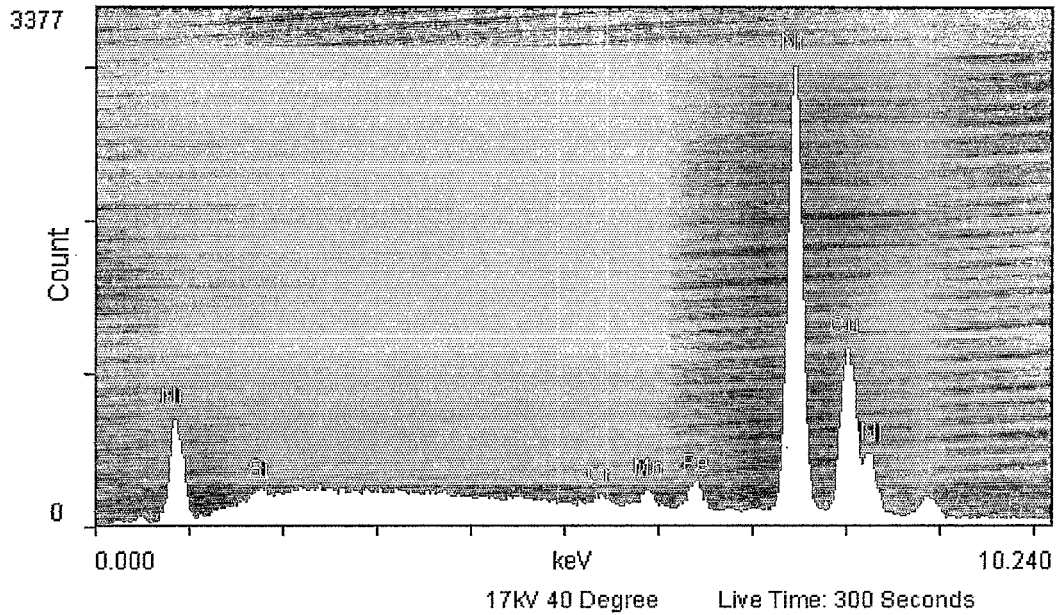


Figure 53e: Last Area of the Fracture Examined by EDS



eV/channel: 10.000
 Acquisition Time(secs): 346
 Number of Channels: 2048
 Low Energy Cutoff(eV): 0
 Digital Offset(channels): 1

Accelerating Voltage: 17 kV	Elevation Angle: 40 dg	Gold Layer: 0.000002 cm
Emission Current: 50 kV	Azimuthal Angle: 22 dg	Dead Layer: 0.000013 cm
Probe Current: 0 nA	Solid Angle: 0 dg	Window Thickness: 0.000035 cm
Diameter of Probe: 0 nm	Incidence Angle: 90 dg	Window Type: 5
Magnification: 100X	Stage Tilt:	Detector Type:

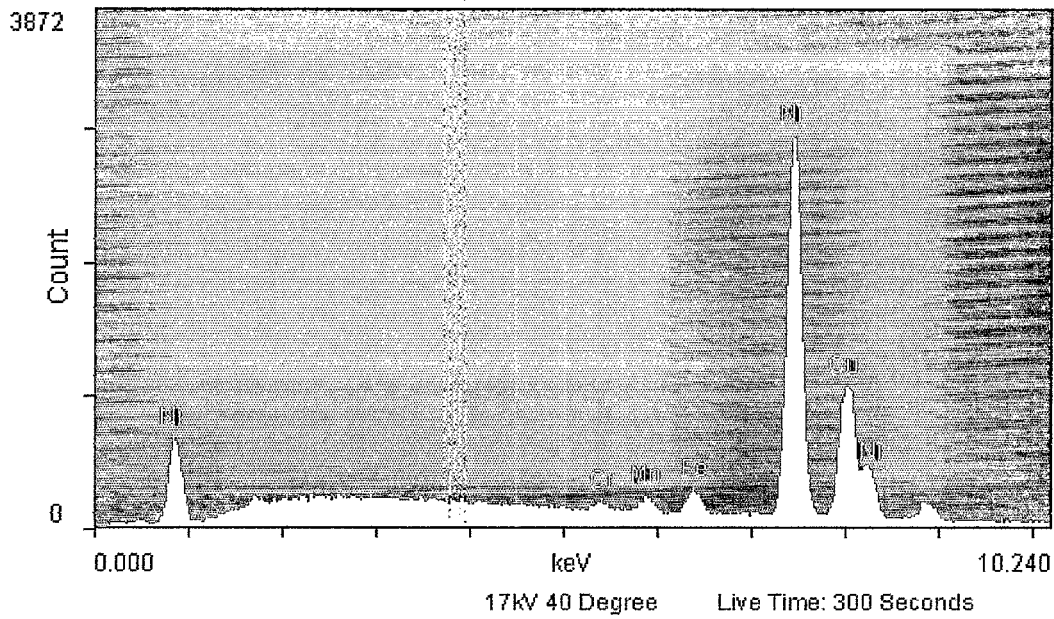
Quantify result: Spectrum 1

ChiSq = 5.32

ZAF Correction

Line	Kratio	Comp	Matrix
Si K	0.007	0.014	2.06
Cr K	0.006	0.006	0.96
Mn K	0.015	0.013	0.90
Fe K	0.011	0.009	0.79
Ni K	0.702	0.696	0.99
Cu K	0.300	0.306	1.02
Total	1.042	1.044	
Elem	WT%	AT%	
Si	1.4	2.9	
Cr	0.5	0.6	
Mn	1.3	1.4	
Fe	0.9	0.9	
Ni	66.7	67.0	
Cu	29.3	27.2	
Total	100.0	100.0	

**Figure 54: EDS Quantitative Analysis of Inco Material.
 Quantify Result: Spectrum 3**



eV/channel: 10.000
 Acquisition Time(secs): 130
 Number of Channels: 2048
 Low Energy Cutoff(eV): 0
 Digital Offset(channels): 1

Accelerating Voltage: 17 kV	Elevation Angle: 40 dg	Gold Layer: 0.000002 cm
Emission Current: 50 kV	Azimuthal Angle: 22 dg	Dead Layer: 0.000001 cm
Probe Current: 0 nA	Solid Angle: 0 dg	Window Thickness: 0.000035 cm
Diameter of Probe: 0 nm	Incidence Angle: 90 dg	Window Type: 5
Magnification: 100 X	Stage Tilt:	Detector Type:

ChiSq = 5.17

ZAF Correction

Line	Kratio	Comp	Matrix
Cr K	0.007	0.007	0.96
Mn K	0.015	0.013	0.90
Fe K	0.015	0.012	0.79
Ni K	0.682	0.676	0.99
Cu K	0.284	0.289	1.02
Total	1.002	0.997	
Elem	WT%	AT%	
Cr	0.7	0.8	
Mn	1.3	1.4	
Fe	1.2	1.3	
Ni	67.8	69.2	
Cu	29.0	27.3	
Total	100.0	100.0	

Figure 55: EDS Spectra of Allvac Material

4.0 DISCUSSION AND CONCLUSIONS

When the evaluation began, the only noticeable major difference between the two heats of material (Inco and Allvac) was in the temperatures to which they were annealed during processing. This provided the basis for the starting point in the test program.

The Inco heat had been annealed at 1725°F, while the Allvac heat had been annealed at 1420-1430°F. This difference provided no definitive conclusions, but it did provide a singular disparity between two samples of the same type of material that behaved differently.

Optical microscopy images taken after all samples were exposed to re-heat treatments revealed pitting and inclusions which EDS analyses identified as magnesium, calcium, and sulfur.

The effects of certain alloying additions to copper based alloys is worth mentioning:

Aluminum is soluble in copper to ~7.8% at elevated temperatures. Alloys with less than ~8% are normally single phase, while as the percentage of aluminum increases to the 9-15% range, the possibility of an alloy capable of a martensitic or eutectoid transformation increases.

Arsenic does not normally cause a welding problem in copper alloys unless nickel is present.

Beryllium can cause an age-hardening reaction with copper (precipitation) and is soluble in copper at 0.3 to 2% depending upon temperature.

Boron strengthens copper and is used as a deoxidizer in copper alloys.

Cadmium usually causes no ill effects during fusion welding of copper alloys since it evaporates from the copper at welding temperatures.

Chromium can form a refractory oxide and in the molten weld pool, since it has such a limited solubility in copper. Chromium can make oxyacetylene welding difficult unless special fluxes are used, and a protective atmosphere is used over the molten weld pool.

Iron issues as the grain refiner in copper alloys. For it has very little effect on weld ability.

Lead is probably the most harmful element when welding copper alloys. It is virtually insoluble in copper at room temperature and is used only to improve machinability. If lead is present in copper alloys they are hot-short and will crack during welding.

Manganese additions are normal in commercial copper alloys. Manganese is highly soluble in copper. It is not detrimental to the welding of copper alloys.

Nickel and copper are completely soluble in each other, in the solid-state, in all proportions. The copper nickel alloys are easily welded, however, they are susceptible to both embrittlement and hot cracking by residual elements.

Phosphorus is used as a strengthener and deoxidizer. It normally does not affect weld- ability of copper alloys as long as it is present in small amounts.

Silicon is used both as a deoxidizer and a major alloying element to improve strength in copper alloys. Copper-silicon alloys have good weldability but they can be hot-short at elevated temperatures. (“Hot-short” is a condition where the metal lacks sufficient ductility and malleability to be worked above the recrystallization temperature.) In welding, the cooling rate for alloys that have significant amount of silicon should be fast enough to prevent cracking in the hot-short temperature range.

Tin can oxidize preferentially to the copper when exposed to the atmosphere during welding operations. This can affect weld strengths because the tin can reduce the strength of the weld due to oxide entrapment.

Zinc is the most important alloying element used commercially with copper. Zinc will evaporates from molten weld metal quite easily.

The minor alloying elements of **Calcium, Magnesium, Lithium, and Sodium** are usually added to copper alloys as deoxidizers. **Antimony** is used to raise the annealing temperature of copper alloys, usually in small enough amount not to affect welding. The alloying additions which may cause hot cracking in copper alloys containing nickel include: **antimony, arsenic, phosphorus, bismuth, selenium, sulfur, and tellurium**. **Carbon**, which is practically insoluble in copper alloys, embrittles these alloys by precipitating in the grain boundaries as graphite.

The cause of the fracture surface oxidation is still open to interpretation, and can be attributed to a number of heat treating operations spanning the entire manufacturing history of the material.

The presence of low melting point elements on the fracture surfaces introduces the possibility of a grain boundary embrittlement issue. This is only a possibility and is not definite, but should be considered.

There was an aggressive etchant reaction from the 1450°F heat treatment sample, which needs to be further considered.

In conclusion, the cause of the failure of the valve body during welding is not yet decipherable, however, it does not appear to be a welding issue. The intergranular fractures indicate a grain boundary problem. The lack of cobalt on the fracture face seems to absolve the stellite weld metal from any grain boundary interaction.

Further examination of the samples using a transmission electron microscope would reveal much more information about the condition of the grain boundaries. This technique can also indicate if there is any graphitization on any boundaries.

No definitive cause of failure could be determined during the analysis conducted for this research.

5.0 RECOMMENDATIONS FOR FUTURE RESEARCH

Further research is recommended in the following areas:

- 1) The structural anomalies observed in the heat-treated specimens need to be characterized. This characterization should take the form of microhardness testing and both scanning electron microscopy and transmission electron microscopy, coupled with energy dispersive spectroscopy. Note: part of the literature survey included two documents supplied by Target Rock personnel [8, 9], which indicate the possibility of second phase formation in the presence of phosphine (PH_3). Phosphine is found in acetylene gas. This anomaly could be an indicator of that second phase.
- 2) The intergranular faceting of the fracture face indicates a structural problem in the material. This also needs to be further evaluated. The possibility of a graphitization process occurring, the potential of a second phase formation, and the constituents/contaminants that may be present in the grain boundaries of this material need to be addressed. This would entail a detailed examination of grain boundaries using the transmission electron microscope coupled with a "hot stage". The hot stage is a TEM specimen holder capable of heating the sample in the TEM, thus allowing concurrent structural examination and heat treatment "in situ". Part of this examination will entail the search for any phosphorous using the SEM and EDS on freshly opened fracture surfaces.
- 3) Another area in need of evaluation is the quantification of the actual effects of phosphine on the second phase formation in these materials. The potential embrittling/corrosive effects and their mitigation are quite important.
- 4) The possible critical importance of the 1450°F annealing temperature, and its potential role in phosphide (Ni or Cu) eutectic formation should also be investigated.
- 5) The use of Auger electron spectroscopy (AES) is also suggested as a tool for future studies of these materials. AES is a method for identification of elemental composition of surfaces. It is based on measuring the energies of Auger electrons. This type of analytical tool lends itself to investigation of fracture surfaces. This is a very narrowly focused technique that might provide significant information on the state of the grain boundary (e.g. contaminants, unusual elements, etc.) in this material. This type of examination was performed by researchers on Alloy K-500 [10,11]. Alloy K-500 is prone to intergranular fracture in both fatigue tests and during hot working. This type of failure has also occurred in K-500 material during room temperature tensile testing. These two references suggest that the K-500 intergranular separation may be due to both Cu segregation to grain boundaries coupled with graphite film formation at the grain boundaries. Both of these conditions were alloy chemistry dependent. Although this is a different alloy, these possibilities should also be investigated for Alloy 400.
- 6) Some work [12,13] has also been performed on the existence of intergranular strains in alloy 400 material. This work indicates that certain crystalline orientations will develop

differing strains during loading. This may allow the “alloy tailoring” of this material, through thermo-mechanical processing techniques. Again, another avenue to pursue.

- 7) Since the grain size [14] also plays a role in mechanical property dependence, work hardening and strain rate effects on grain boundaries in Alloy 400 should be evaluated. The purchase specification for manufacture of this material should specify the smallest grain size possible to obtain the minimum mechanical and weldability properties. During the visits to TRC, it appeared that grain size maximum values were not measured. This is perhaps another area to be investigated with this material (grain size dependence versus cracking susceptibility during welding).

Immediate Recommendations:

Since the literature review indicates that there is a potential corrosive effect of phosphorous compounds on the Ni-Cu material, TRC should evaluate what sources might exist for their introduction into the welding/hard-surfacing processes. These sources should be evaluated and eliminated, if possible. This would include cutting oils, solvents, and gas mixtures.

6.0 REFERENCES

1. <http://www.jwharris.com/jwref/faq>, July 9, 2001.
2. H.B. Cary, “Modern Welding Technology,” Prentice-Hall, New Jersey, 1979.
3. P. Crook, Cobalt and Cobalt Alloys, in *Properties and Selection: Nonferrous Alloys and Special-Purpose Materials*, Vol 2, 10th ed., *Metals Handbook*, ASM International, 1990, p. 446-454.
4. Heat A, Certified Material Test Report No. 72786, INCO Alloys International.
5. Heat B, Certificate of Test for Heat KG96, ALLVAC.
6. Specification MIL-N-24106 Revision C.
7. <http://www.webelements.com>, July 30, 2001.
8. Scrimgeour, N., McLeish, J.A., McKeown, D., Scott, M.H., “Hard Facing and Dissimilar Weld Metal Welding of Monel Alloy 400. Part 1. Hard Facing of Monel Alloy 400”, *Welding and Metal Fabrication*, January/February 1975.
9. Scrimgeour, N., McLeish, J.A., McKeown, D., Scott, M.H., “Hard Facing and Dissimilar Weld Metal Welding of Monel Alloy 400. Part 2. Dissimilar Metal Joints”, *Welding and Metal Fabrication*, March 1975.

10. Cao, W-D., Kennedy, R.L., Choudhury, A., "Auger Electron Spectroscopy Study Of Grain Boundary Segregation In Alloy K-500: Part I. Behavior In As-Processed State", Metallurgical Transactions A, Vol. 24A, September 1993, p.1897-1907.
11. Cao, W-D., Kennedy, R.L., Choudhury, A., "Auger Electron Spectroscopy Study Of Grain Boundary Segregation In Alloy K-500: Part II. Behavior In Slow Strain Rate Tensile Test", Metallurgical Transactions A, Vol. 24A, September 1993, p.1909-1917.
12. Holden, T.M., Clarke, A.P., and Holt, R.A., "Neutron Diffraction Measurements of Intergranular Strains in Monel-400", Metallurgical and Materials Transactions A, Volume 28A, December 1997, p. 2565-2576.
13. Holden, T.M., Tome, C.N., and Holt, R.A., "Experimental and Theoretical Studies of the Superposition of Intergranular and Macroscopic Strains in Ni-Based Industrial Alloys", Metallurgical and Materials Transactions A, Volume 29A, December 1998, p. 2967-2973.
14. Gray, G.T. III, Chen, S.R., and Vecchio, K.S., "Influence of Grain Size on the Constitutive Response and Substructure Evolution of Monel 400", Metallurgical and Materials Transactions A, Volume 30A, May 1999, p. 1235-1247.